Summer 2018

The Effect of Soxhlet Extraction and Synthesis Temperature on Properties of Polyaniline

Samuel Watson Stahl
Old Dominion University, swstahl@odu.edu

THE EFFECT OF SOXHLET EXTRACTION AND SYNTHESIS TEMPERATURE ON PROPERTIES OF POLYANILINE

By

Samuel Watson Stahl
B.S. May 2016, James Madison University

A Thesis Submitted to the Faculty of
Old Dominion University in Partial fulfillment of the
Requirements of the Degree

MASTER OF SCIENCE

CHEMISTRY

OLD DOMINION UNIVESITY
August 2018

Approved by:

Richard Gregory (Advisor)

Ken Brown (Member)

Bala Ramjee (Member)

Hani Elsayed-Ali (Member)

ABSTRACT

THE EFFECT OF SOXHLET EXTRACTION AND
SYNTHESIS TEMPERATURE ON PROPERTIES OF POLYANILINE

Samuel Watson Stahl
Old Dominion University, 2018
Advisor: Dr. Richard V. Gregory

Polyaniline was synthesized by the chemical oxidation of aniline in an HCl solution by ammonium persulfate. The temperature of the synthesis was varied to increase the molecular weight of the polymer from 37,600 Da to 52,400 Da. Soxhlet extraction using methanol as the primary solvent was performed on half the sample in order to further increase the average molecular weight by approximately 3150 Da and decrease the polydispersity index by 0.8. Films were cast from 1,3-dimethyl-3,4,5,6-tetrahydro-2(1H)-pyrimidinone (DMPU) and *N*-methyl-2-pyrrolidone (NMP) and then doped with trifluoromethanesulfonic acid.

The effect of the soxhlet extraction and synthesis temperature on the polymer's properties were analyzed. Among the properties examined were thermal events, crystallinity, molecular weight, electrical conductivity, and infrared spectra. Soxhlet extraction proved useful in rinsing out not only short chain oligomers, but also residual solvent and dopant. This lack of solvent and oligomers proved advantageous to the properties of the polyaniline films, resulting in films that were more conductive and of higher crystallinity since higher molecular weight polymers have larger crystal domains. An unexpected result of the extraction was that the polymer powder showed a resilience to solid state crosslinking, an irreversible process which occurs at approximately 150°C which decreases the conductivity of the polymer by orders of magnitude.

Decreased synthesis temperature also proved advantageous, producing polymer of significantly higher molecular weight. Films made from polymer synthesized at room temperature resulted in films which were brittle and cracked easily upon doping. This mechanical shortcoming resulted in films which were much less conductive than films cast from polymer synthesized at low temperature. The increased temperature and heat required for crosslinking was also observed for samples synthesized at lower temperatures.

This thesis is dedicated to my loving family.
Thank you for helping me through two decades of education
and teaching me the value of hard work.

ACKNOWLEDGEMENTS

Firstly, I would like to thank Dr. Gregory for accepting me as a graduate student and guiding me through this research project. I would also like to thank the members of my committee for their assistance through this research. I would like to thank the two institutions which made this research possible, Old Dominion University for allowing me to perform syntheses, DSC, and TGA as well as the Applied Research Center at Jefferson Lab for allowing me to perform XRD, FTIR, and conductivity tests on their premises. Thanks must also be extended to my peers at Old Dominion, in particular Kory Castro, Storm-Marie Allmon, Sean Downs, and Andrew Benedict. I would also like to thank the Georgia Tech Research Institute for their GPC analysis.

TABLE OF CONTENTS

Page

LIST OF TABLES

Table Page

LIST OF FIGURES

Figure Page

CHAPTER 1
INTRODUCTION

Due to their easy processability, relatively light weight, and versatile mechanical properties, polymers have received a great deal of attention for a number of applications. Long before the realization of their chemical structure, polymers have been used in various forms such as textiles and fibers. The versatile nature of polymers was further enhanced with the advent of man-made and synthetic polymers and is still being expanded on today. One of the most profound polymeric discoveries of the twentieth century was that some polymers could conduct electricity. This was a serendipitous discovery by the Shirakawa lab when an excessive amount of catalyst was used in the synthesis of polyacetylene which resulted in a black film which was mildly electrically conductive [2]. This class of organic conductors and semiconductors has since been termed Intrinsically Conductive Polymers (ICPs) and have replaced their inorganic counterparts in a number of applications such as lasers, electro-optic devices like solar cells, semiconductors, electronics, and sensors for both biological and chemical analytes.

ICPs are polymeric materials which conduct electricity without additives. This definition excludes extrinsically conductive polymer composites: non-conductive polymer combined with additives such as polycarbonate / stainless steel composites [3]. A number of polymers have been shown to be intrinsically conductive, a few of which are shown in **Figure 1**. There are several advantages to these ICPs compared to their inorganic counterparts. One advantage is their low density which leads to more lightweight electronics. The ability to create lightweight electronics is imperative for extraterrestrial exploration where every kilogram of cargo requires thousands of dollars to put in orbit [4]. For example, the first manned mission to mars will require an expansive

Figure 1

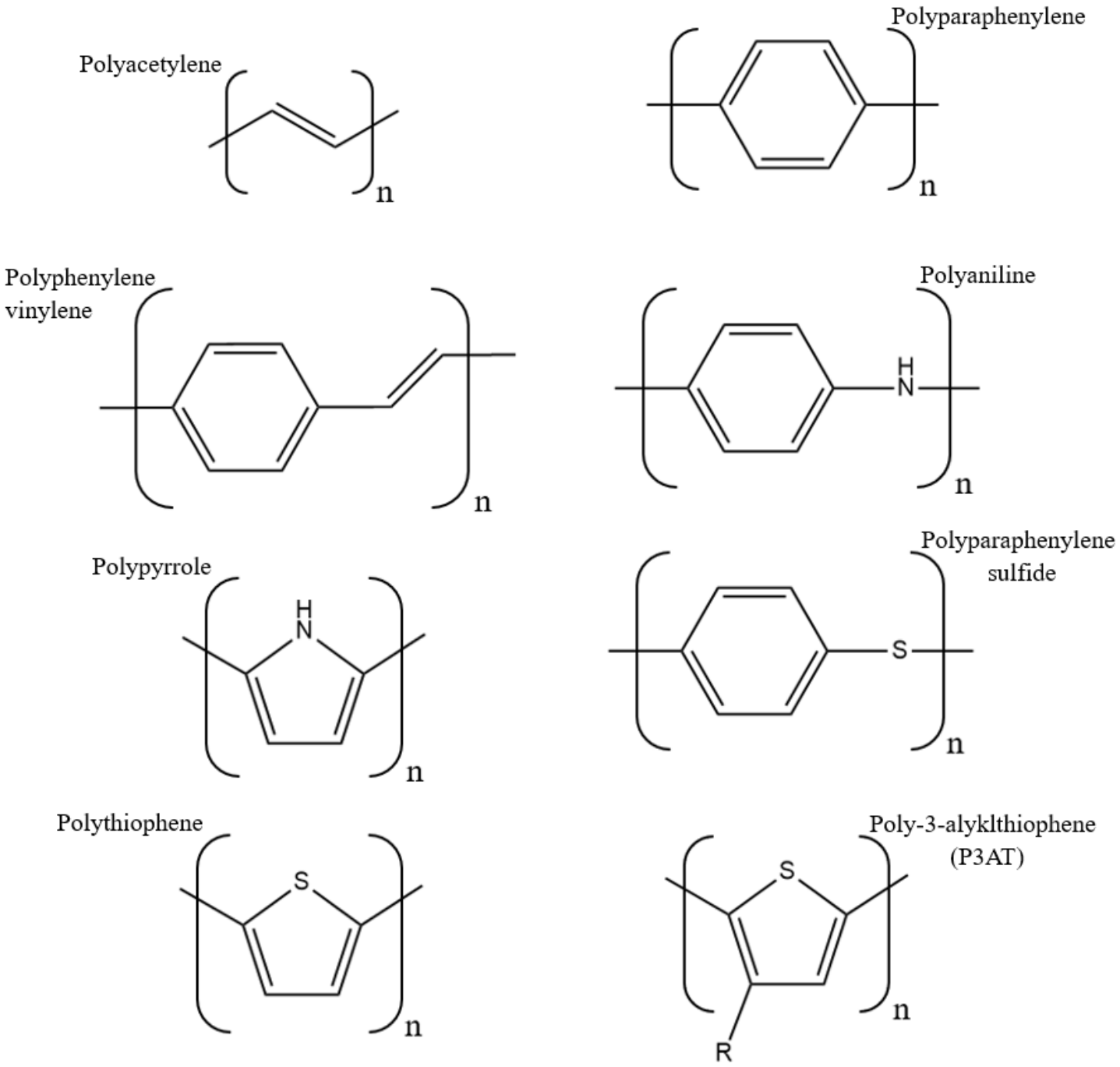

Figure 1. Structures of commonly used conducting polymers

solar array to provide the necessary energy. The cost of transporting these solar cells will decrease substantially if organic or hybrid solar cells are used. Another advantage ICPs have over inorganics is their flexibility. Flexibility allows for ICPs to be coated onto existing fibers or spun into fibers themselves which are ideal for wearable electronics such as biosensors. A third advantage of ICPs is their tunable conductivity which makes ICPs ideal candidates to be used for optical applications such as organic LEDs and solar cells.

The main drawback to ICPs is that they are difficult to process since ICPs typically do not melt and have limited solubility. Both of these characteristics arise due to the conjugated π electron system present in the polymer backbone, a trait which is absolutely necessary for the transport of electrons through the system. The conjugated π system results in rigid polymer backbones which ash before gaining the thermal energy to slip past each other. This means that most ICPs typically do not have thermal transitions such as a melting point or glass transition point. The conjugated π system also results in a strong π – π stacking interactions between neighboring chains [5]. While this attraction is imperative for the conduction mechanism of ICPs, it also results in chains that are difficult to separate via solvation.

One way around the issue of solvation is the addition of side chains. An example of this can be found in **Figure 1** when comparing polythiophene and poly-3-alkylthiophene (P3AT). It can be seen that both polymers share the same polythiophene backbone, the difference being the additional side chains of P3AT. The purpose of the side chains is to give organic solvents a site to interact with, essentially a "handle" on an otherwise insoluble backbone. The most common example of P3AT has the addition of a hexyl group (R= $-C_6H_{13}$) yielding the polymer poly-3-hexylthiophene (P3HT). P3HT is much more easily processable, increasing the solubility from

essentially none to 84.1 mg/ml in some solvents [6] without changing the band gap of polythiophene [7-8].

A third problem with ICPs is their reactivity in ambient atmosphere. When oxygen is introduced into the system the conjugated π backbone is disturbed and the conductivity suffers as a result. For example, P3HT synthesized under an inert atmosphere has electron mobility of approximately 0.1 $cm^2/V\ s$ [9] while the same polymer synthesized under ambient atmosphere had a much lower mobility of 0.045 $cm^2/V\ s$ [10]. This trend has also been observed with exposure of P3HT devices to atmospheric conditions. In one study observing the behavior of P3HT for possible application in solar cells, P3HT lost 95% electron mobility after being stored in ambient, dry atmosphere for 18 days [11]. Polythiophenes made with varying synthesis methods and side chains have been developed to overcome this instability, but there is always a tradeoff between electron mobility and stability in air [12-14].

An alternative to permanently modified polymers like P3AT is a polymeric system that can be reversibly switched between a soluble, nonconductive form and a form which is conductive but not easily processable. Polyaniline (PANI) offers such a solution. In addition to its ease of processability, PANI also shows stability under atmospheric conditions. First discovered in 1862 during an investigation of nitrobenzene poisoning, its utility was not realized until it was doped to its semi-conductive state in the early 1980s [15-16]. Since then, PANI has become widely used for a variety of applications including devices such as battery cathodes, supercapacitors, and chemical sensors [17-19]. The conductivity of PANI relative to other common materials and ICPs can be compared in **Figure 2**.

Due to the novelty of PANI, there are still some aspects of preparation which need further investigation. An example of this is synthesis temperature. Many studies use PANI synthesized

at sub-zero temperatures while other studies polymerize at room temperature [20-21]. Even among researchers that perform temperature-controlled synthesis, there is no agreed-upon temperature.

PANI is made up of alternating benzoid rings and nitrogen atoms which are in the *para* positions of the benzoids. A general structure can be seen in **Figure 1**. The mechanism of aniline

Figure 2

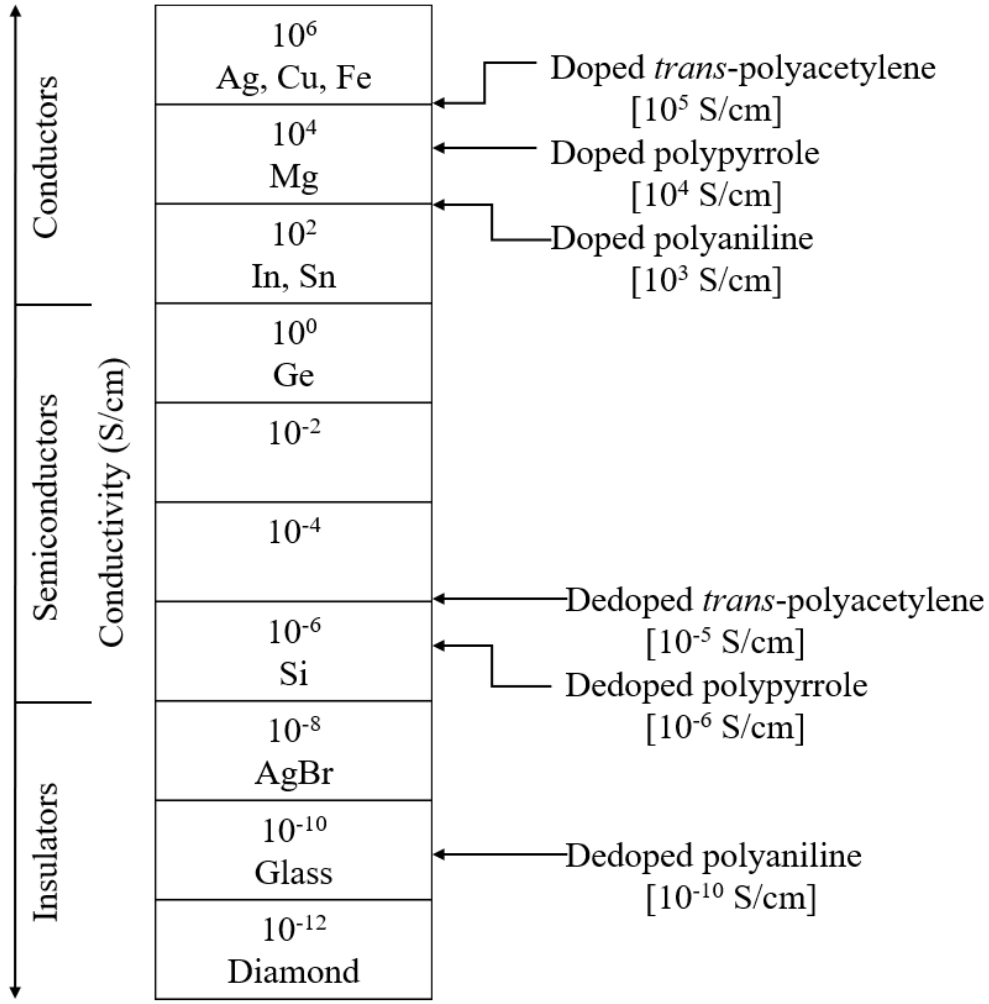

Figure 2. Comparison of the conductivity of a few ICPs to the conductivity of common materials. This figure was modified from the third edition of The Handbook of Conducting Polymers, Chapter 15 [5].

polymerization can be broken down into three general steps: initiation, dimerization, and propagation. The polymerization reaction has been shown to be surface catalyzed, meaning PANI will first polymerize on available surfaces before precipitating in solution [22]. In the absence of a suitable surface, aniline monomers will initiate the polymerization and form aniline dimers and then oligomers which quickly become insoluble as chain length increases. These aniline oligomers become solid particulates, the surface of which catalyzes PANI propagation. Oxidized aniline now has two pathways: kinetically favorable propagation of existing polymer chains or unfavorable initiation of a new aniline dimer. When considering the PANI synthesis mechanism one cannot overlook the possibility of defects such as the *ortho* coupling of aniline [23] and the initiation of side chains onto non-terminal rings [24]. When considering the kinetics of aniline polymerization and its side reactions, it suggests that lower temperatures should result in longer polymer chains with fewer defects.

Another step in the production of PANI used by many researchers is soxhlet extraction. Soxhlet extraction is a method of washing the solid PANI powder with a solvent which readily dissolves low molecular weight PANI but not high molecular weight PANI. The theory behind a soxhlet extraction is that the solvent will wash out short chain oligomers while leaving the longer polymer chains.

In this study, both of these aspects of PANI preparation were investigated. The objective of this research will be to explore variations in synthesis temperature to observe the dependence of various characteristics including crystallinity, polymer weight, electrical conductivity, and thermal properties. A second variable which will be explored is the effect of soxhlet extraction. The hope of this study is to develop more reproducible pathways for polyaniline synthesis.

CHAPTER 2

LITERATURE REVIEW

Reversible Oxidation/Reduction of Polyaniline

Polyaniline describes a class of polymers of the general composition

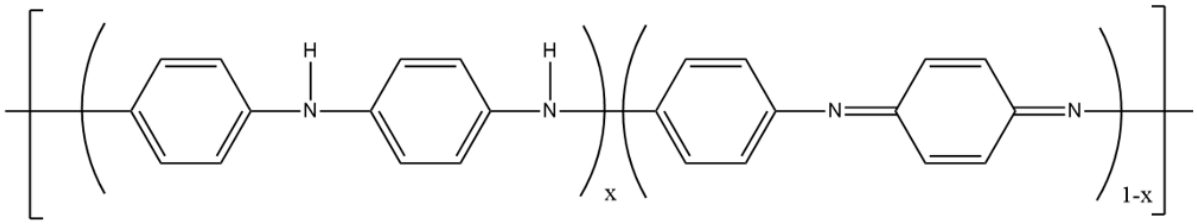

which is comprised of two repeat units:

Reduced:

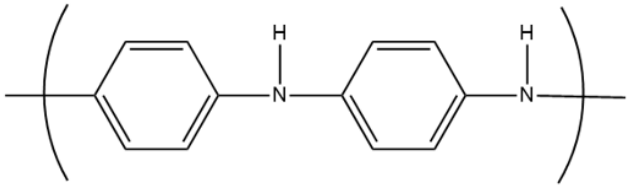

Oxidized:

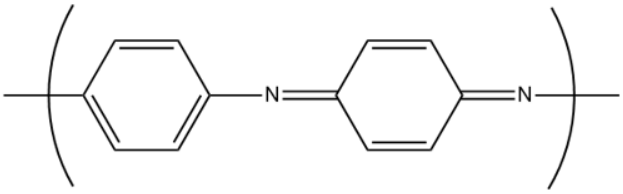

Pure PANI has three forms depending on the ratio of reduced/oxidized repeat units: leucoemeraldine base, emeraldine base, and pernigraniline base which correspond to x = 0, 0.5, and 1 respectively. In addition to these three forms consisting of only polyaniline, a third form exists known as emeraldine salt which is created when EB is exposed to an acidic dopant. PANI

can easily be converted between any of these forms and each form has different characteristics. The reversible nature of PANI can be seen in **Figure 3**.

Leucoemeraldine base (LEB) is the most reduced form of PANI, being comprised of alternating phenyl rings and tertiary amines. Due to the lack of a conjugated π backbone, LEB is an insulator with a conductivity of 10^{-10} S/cm and a band gap of 3.57 eV [25]. While not conductive, LEB is much more easily processable than most other ICPs due to its high solubility and definable melting point [26-27]. While LEB is stable in solution, it quickly forms an oxide layer when exposed to ambient atmosphere. Surprisingly little work has been done on LEB compared to PANI's more popular emeraldine base and emeraldine salt forms.

Pernigraniline base (PNB) is the most oxidized form of PANI which is comprised of alternating phenyl/quinoid rings separated by secondary amines. Having a completely conjugated π backbone, PNB lies in the semiconductor range with a band gap of 2.3 eV [28]. While this form of PANI does seem potentially useful, PNB quickly and spontaneously degrades back to emeraldine base which limits its applications.

Figure 3

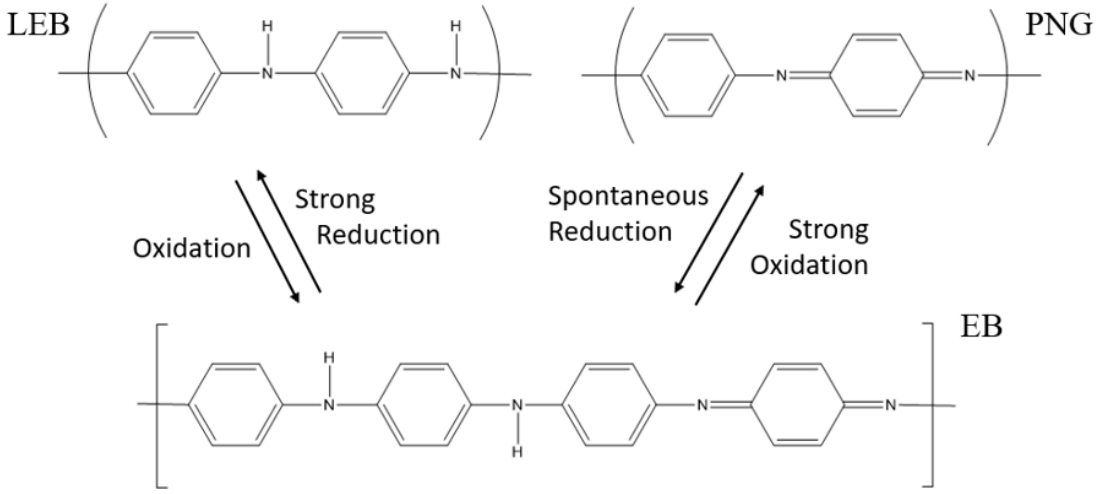

Figure 3. Reversible nature of PANI between its various oxidation states.

Emeraldine base (EB) is by far the most popular oxidation form of PANI in research and device fabrication. Like LEB, EB does not have a fully conjugated π backbone resulting in an insulating material with a band gap of 3.60 eV [29-30] and conductivity on the order of 10^{-9} S/cm [31]. Although not electrically conductive, EB is the most easily processable form of PANI since EB is stable under atmospheric conditions. EB is also soluble in solvents such as *N*-methyl-2-pyrrolidinone (NMP), capable of solubilize 10% weight EB for 60 minutes without gelation, and thermodynamically superior 1,3-dimethyl-3,4,5,6-tetrahydro-2(1H)-pyrimidinone (DMPU), capable of solubilizing 17.5% weight EB for 400 minutes without gelation [26]. This gelation is due to crosslinking of the polymer backbone and will be discussed in subsequent sections. Due to its atmospheric stability and relatively high solubility EB has been used as an intermediate to fabricate a variety of devices such as strain gauges and pH monitors, field effect transistors, and conductive film material for circuit boards which can be used once the EB is easily doped into ES [32-34].

Emeraldine salt (ES) is the form of PANI of interest as an ICP. ES has a small band gap of 1.5 eV which results in a conductivity of 350 S/cm or greater, 11 orders of magnitude higher than any other form of PANI [35-36]. This transition between insulator to semiconductor occurs without any change of electrons on the polymer chain, instead adding hydrogen ions to the backbone of the polymer chain to induce the charge, a process which can be seen in **Figure 4**. Once the imine nitrogen has accepted the hydrogen and positive charge, the quinoid-imine double bond will rearrange resulting in a benzoid and cationic nitrogen radical. This cationic radical is called a hole and can be thought of as the equivalent to a positively charged electron. Once induced, the hole is distributed a short distance along the polymer backbone, typically no more than 20 monomer units [37]. The theory relating these radicals and conductivity will be

Figure 4

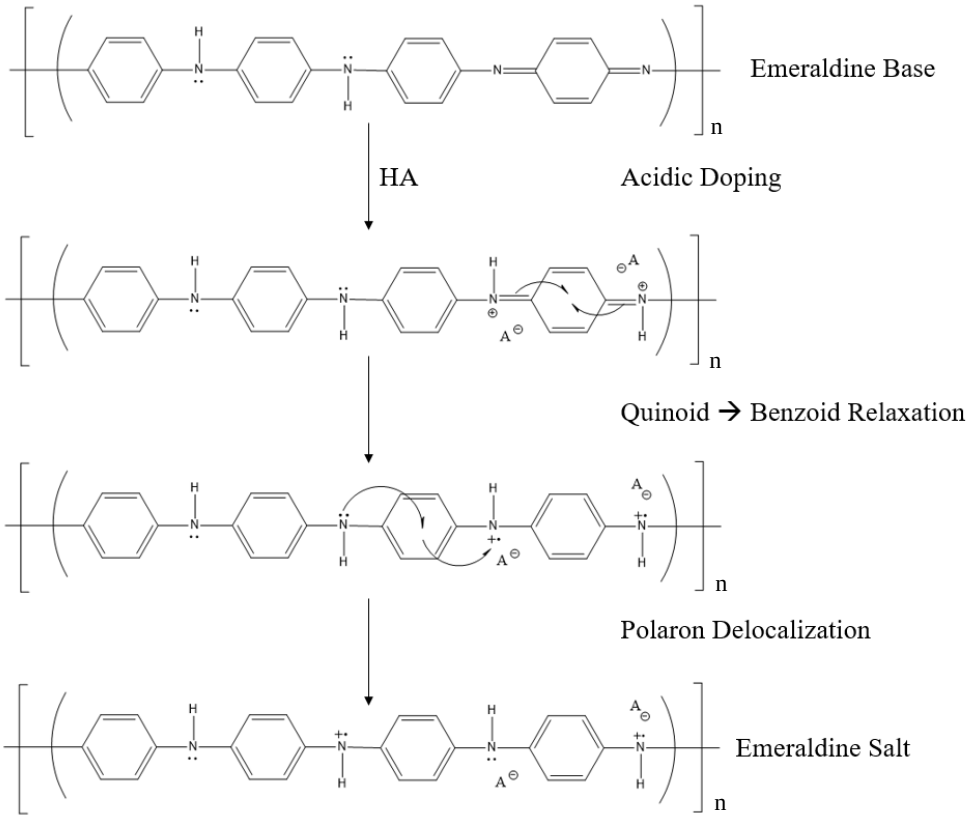

Figure 4. Mechanism of polaron formation of PANI from its EB form.

discussed in the subsequent section. The drawback of ES is that it is much more difficult to process than its undoped counterpart, EB. The degree of solubility is largely dependent on the anionic dopant of the ES. For example ES doped with HCl is completely insoluble in DMF, but if doped with toluene-*p*-sulfonic acid the solubility increases dramatically [38].

Band Theory of Solids

The theory behind the conductivity of ICPs is called Band Theory and is based on the molecular orbitals of the polymers. While quantum aspects of the charge carriers are important, classical Band Theory describes the conduction mechanism. In order to build the molecular

Figure 5

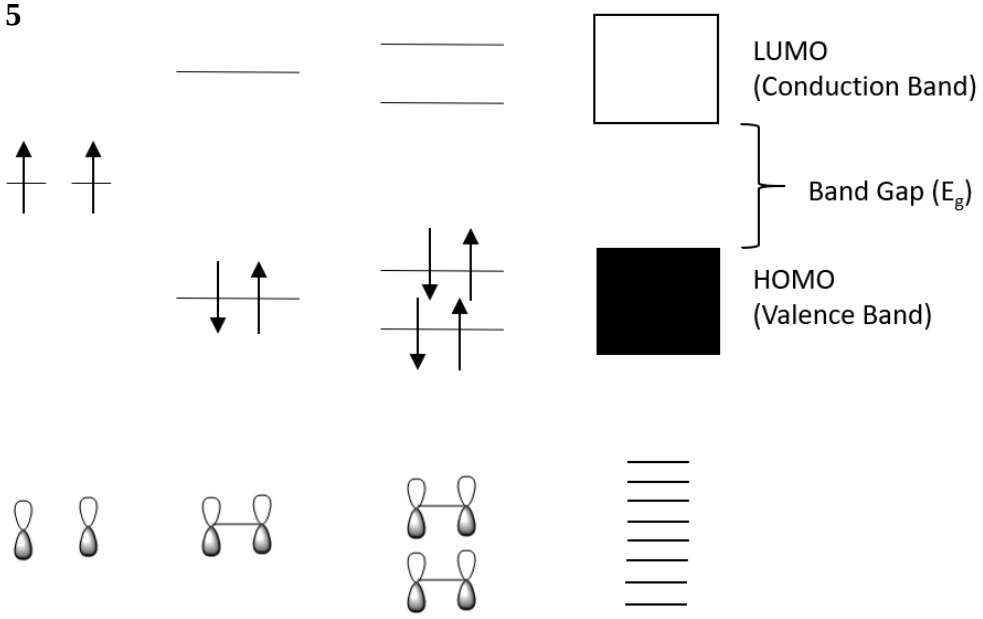

Figure 5. The transitions from discrete energy levels of stacked ethylene molecules to the relatively wide bands through which electrons can move.

orbital, one can first imagine a pair of carbon atoms sharing no elections. When bound in a single ethene molecule, the electrons create several energy states to be populated by elections including the HOMO and the LUMO: π and π* respectively. When another ethylene molecule is brought in close proximity, the orbitals interact forming two π and two π* energy states. When a sufficient number of ethylene molecules are stacked, the energy states act less like discrete orbitals and more like a series of bands in which electrons can move freely. In standard MO theory these would be considered the HOMO band and the LUMO band while in Band Theory they are called valence band and conduction band respectively. The distance between the two bands is the band gap (E_g) and represents the energy required to move an electron from the valence band to the conduction band. The fermi level is located midway between the valence and conduction bands. The transition between molecular orbital theory and band theory can be seen in **Figure 5**.

Figure 6

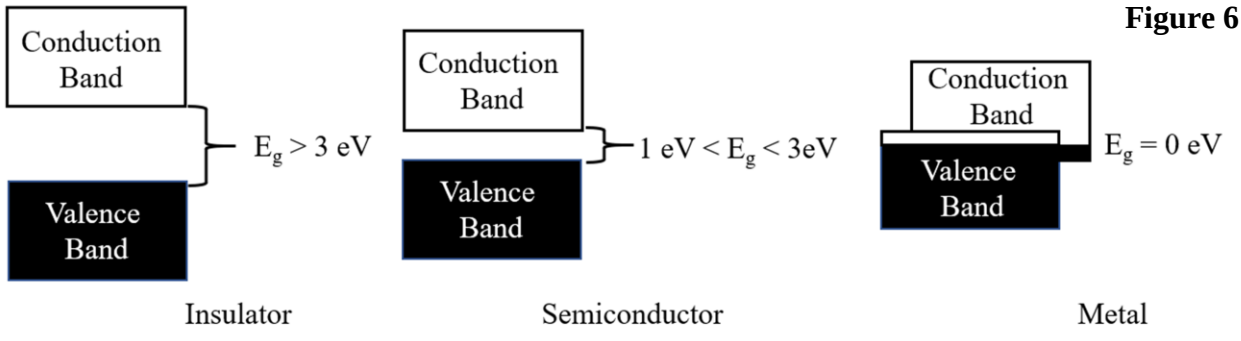

Figure 6. Comparison of the band gaps of insulators, semiconductors, and metals. Note that in the overlapping bands of metals, both the conduction band and the valence band are partially filled allowing the material to be electrically conductive with no energy input.

At this point, Band Theory acts much like molecular orbital theory for inorganic semiconductors: conductivity cannot occur when both the HOMO and LUMO are completely filled or empty. In order to turn on the conductivity, an electron from the valence band must be given the energy to be promoted to the conduction band, the band gap energy. This concept is what links band gap and conductivity. Materials with a band gap greater than 3 eV are insulators, materials with a band gap between 1 eV and 3 eV are semiconductors, and materials with a band gap less than 1 eV are conductors. Some materials have valence and conduction bands which overlap, in other words a band gap of 0 eV, and are metallic conductors. This overlap indicates that both bands are partially filled with no energy input required. It should be pointed out that the conduction method is different between metals and semiconductors, for example the effect of temperature on conductivity. In semiconductors, increasing temperature promotes more electrons into the conduction band giving a positive correlation between temperature and conductivity [39]. The reverse is true for most metals, increasing temperature having no effect on the distribution of electrons in the valence and conduction bands since no energy is required for electrons to go

between the two. Instead of promoting conductivity, increased temperature causes lattice vibrations in metals which disrupt the electron's path causing a negative correlation between temperature and conductivity [40]. A comparison of band distances can be seen in **Figure 6**.

Effect of Dopant on Conductivity

The band gap can be decreased by doping. When EB is doped to ES, the destabilized bonding orbital is expressed as a new energy state between the valence and conduction bands called a polaron. This polaron acts like a stepping stone, decreasing the energy required for the electron to be promoted into the conduction band and turn on electrical conductivity.

There are several types of polarons which can be used to turn on the conductivity of ICPs. The polaron described previously for PANI is a cationic radical and is comparable to a p-type semiconductor. When an electron is removed from the top of the valence band, the electron's pair will relax into an energy state outside of the valence band [37]. This new energy state creates a virtual energy level located between the valence band and the fermi level. When many polarons are formed in a system, the virtual energy states overlap and form a continuous energy band. It is also possible to introduce an anionic radical to the conjugated polymer backbone. The added electron is not injected directly into the conduction band, as one would assume from inorganic semiconductor doping, but relaxes into a new energy level between the fermi level and the conduction band. Though theoretically as useful as the cationic polaron, anionic polarons are less stable which makes them less popular for practical and academic purposes [41]. If a cationic polaron is further oxidized it is possible to create a system in which the two holes act as a single unit called a bipolaron. A parallel process can occur when an anionic

polaron is further reduced. The virtual energy states which arise from these cationic and anionic bipolarons are of similar energies as their singly charged counterparts but lie slightly closer to the fermi level.

Polarons differ from bipolarons by their spin. Because polarons are formed due to radical ions, the spin of the unpaired electron is not negated resulting in a spin of ½. Bipolarons are formed from a pair of electrons being added or removed. With both the spin up and spin down electrons removed, the overall spin of the system is zero. The electron distribution in undoped, polaronic, and bipolaronic semiconductors can be seen in **Figure 7.** Polarons have been shown to be the method of conductivity for PANI by electron spin resonance (ESR) studies [42]. Other ICPs use different polaronic states depending on their structure. For example polythiophenes are more

Figure 7

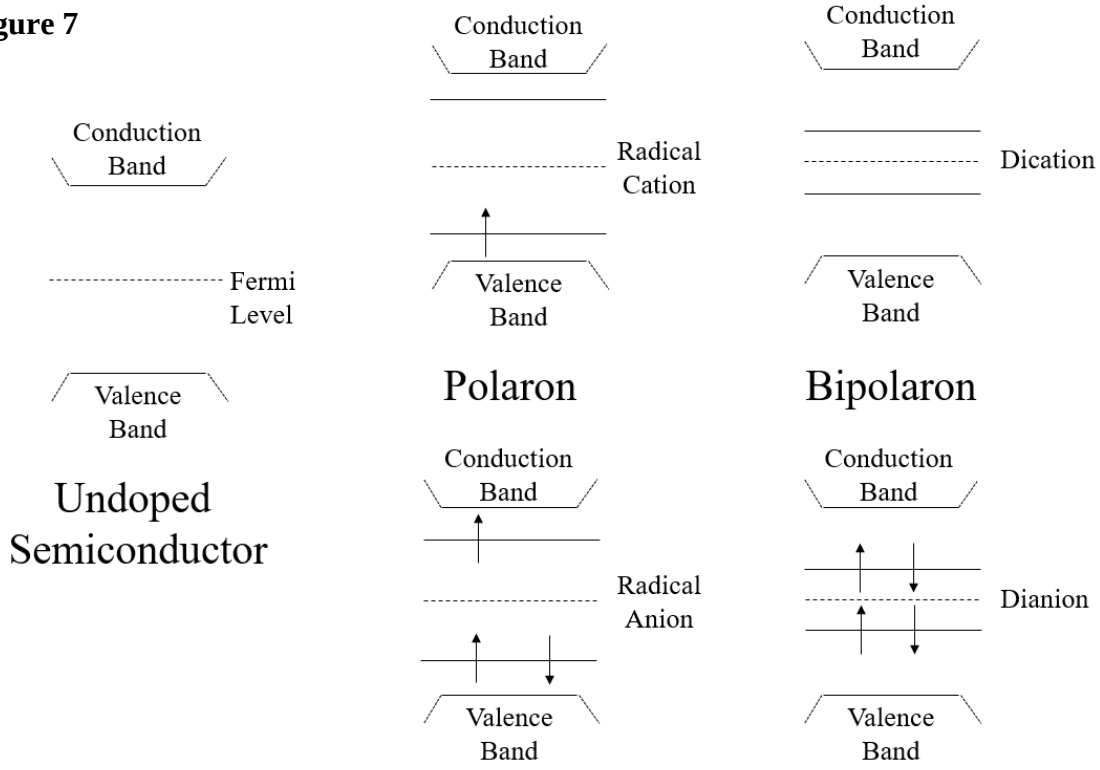

Figure 7. The locations of polaron bands relative to the existing band gap.

stable in a bipolaronic state as observed in both experimental and theoretical studies [43,44]. Still other ICPs switch between polaronic/bipolaronic states depending on the strength of the electric field. An example of this is doped poly (para-phenylene) which exhibits polaronic states below an electric field strength of 1.5 (±0.1) mV/Å and bipolaronic states above an electric field strength of 1.5 (±0.1) mV/Å [45].

Polymerization Mechanism

The procedure for the chemical synthesis of polyaniline is well agreed upon among researchers [46-48]. An aniline solution is made in acidic medium. An acidic medium is used to make the aniline more soluble and better control the synthetic pathway. At this point some researchers chill the acidic aniline solution while others perform the synthesis at room temperature. As previously mentioned, even among low temperature synthesis there is no agreed upon temperature at which to create reproducible polyaniline. Once the aniline solution is at the desired temperature, a solution of ammonium persulfate (APS) is added. Some syntheses add the entire solution of APS at once while others add the oxidizer over a period of time. APS oxidizes the aniline which begins the polymerization. APS addition continues until a molar excess of APS compared to aniline has been added. With the plethora of variations on PANI synthesis, it is little wonder that the quote by Professor A.G. MacDiarmid that "there are as many different types of PANI as there are people who synthesize it" has become a commonly parroted opinion.

While the procedure for polyaniline synthesis is very straightforward, the mechanism behind the synthesis is still debated. In this work the polymerization mechanism for PANI will be broken down into three steps: initiation via aniline oxidation, dimerization, and propagation.

Figure 8

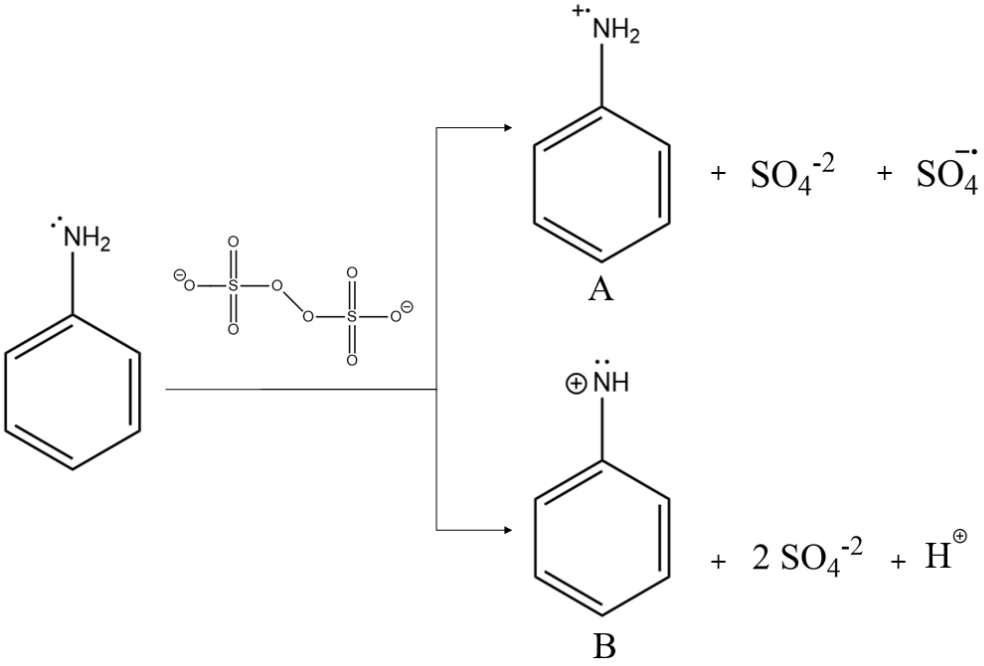

Figure 8. Two proposed products for the oxidation of aniline by APS: A) aniline cationic radical and B) aniline nitrenium cation.

Many investigators believe that the initiation reaction for PANI synthesis involves the oxidation of a single electron from aniline by APS to form aniline cationic radical (**Figure 8** A) [49-51]. While this is undisputed for single-electron oxidants such as Fe(III), the peroxydisulfate anion is a very powerful electron acceptor with a redox potential of +2.0 V versus NHE. Peroxydisulfate can act as a single-electron oxidizing agent, as with Fe(II):

$$Fe^{+2} + S_2O_8^{-2} \rightarrow Fe^{+3} + SO_4^{\bullet -} + SO_4^{-2}$$

or as a two-electron oxidizing agent, as with Pb(II):

$$Pb^{+2} + S_2O_8^{-2} + 2H_2O \rightarrow PbO_2 + 4H^{+} + 2SO_4^{-2}$$

depending on the nature of the species being oxidized [52]. There is computational evidence supporting the theory that APS acts as a two-electron oxidant based on the fact that the sulfate anionic radical is also a very powerful oxidizer with a redox potential of 2.5 – 3.1 versus NHE.

Studies indicate that it is more thermodynamically stable for the sulfate anionic radical to further oxidize the aniline cationic radical producing the aniline nitrenium cation (**Figure 8** B) after the loss of a hydrogen ion [53-54]. Experimental evidence against the formation of a radical cation is presented by Behrman *et al*. in a study which showed that oxidation of aromatic amines with peroxydisulfate is not hindered by the presence of a radical trap, a species which would have halted any radical reaction [55].

Dimerization is a critical step in the polymerization process with numerous outcomes depending on the conditions at which the reaction occurs. Some of the possible dimerization products can be seen in **Figure 9.** The products are often described by the two sites which bonded to create it: the nitrogen being the "head" and the 4-position of the phenyl ring being the "tail." For example, 4-aminodiphenylamine (4-ADPA) (**Figure 9** C) is the product of a "head to tail" coupling while side product benzidine (**Figure 9** D) is the product of "tail to tail" coupling. In an ideal situation, 4-ADPA would be the only product since all other structures lead to defects in PANI chains. Both possible forms of APS oxidized aniline (molecules A and B) form neutral 4-ADPA through a head-to-tail reaction with aniline followed by the loss of two H^+ ions for aniline cationic radical and a single H^+ ion for aniline nitrenium cation. The prevalence of each dimerization product has been shown to be dependent on pH. The preferred 4-ADPA has been shown to be the dominant dimer under acidic conditions while hydrazobenzene is dominant in more basic solutions [56]. Formation of benzidine via tail to tail dimerization becomes more frequent with increasing acidity: having negligible concentrations above pH 4, over 20% compared to 4-ADPA at pH less than 1, and nearly 50% in super acidic conditions of pH -2 [57]. Formation of azo compounds via head to head coupling show an inverse relationship to pH, their concentrations becoming more prevalent at more alkaline pH [58]. It should be noted that these

trends have been observed in experiments using electrochemical methods. Little work exists on aniline dimerization using solution-based methods [52].

The mechanism for the propagation of polymer chains is fairly well agreed upon. Once aniline (AN) dimer has been formed, it is oxidized again and the chain builds onto it resulting in a stepwise oxidative polymerization. Due to the extended π/n electron system in aniline oligomer

Figure 9

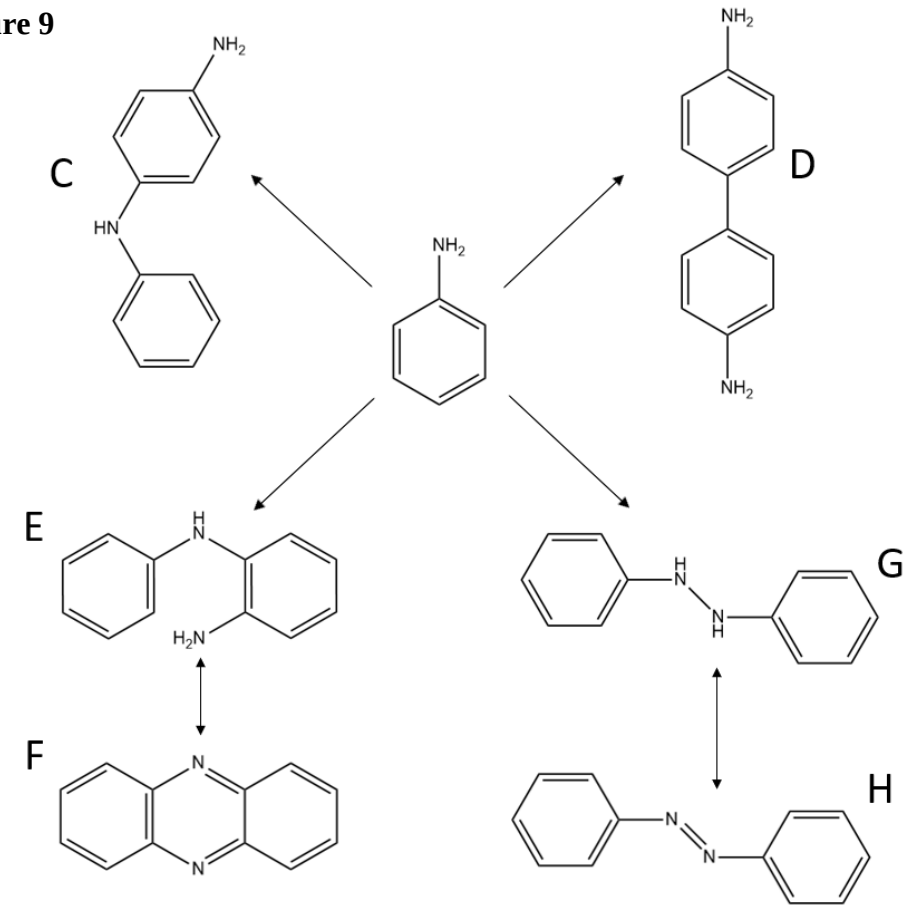

Figure 9. Possible pathways for the oxidative dimerization of aniline. These are the products which have been observed with the chemical oxidation of aniline, many more have been observed when aniline is oxidized by electrochemical methods. The products are C) 4-aminodiphenylamine, D) benzidine, E) 2-aminodiphenylamine, F) phenazine, G) hydrazobenzene, H) azobenzene.

Figure 10

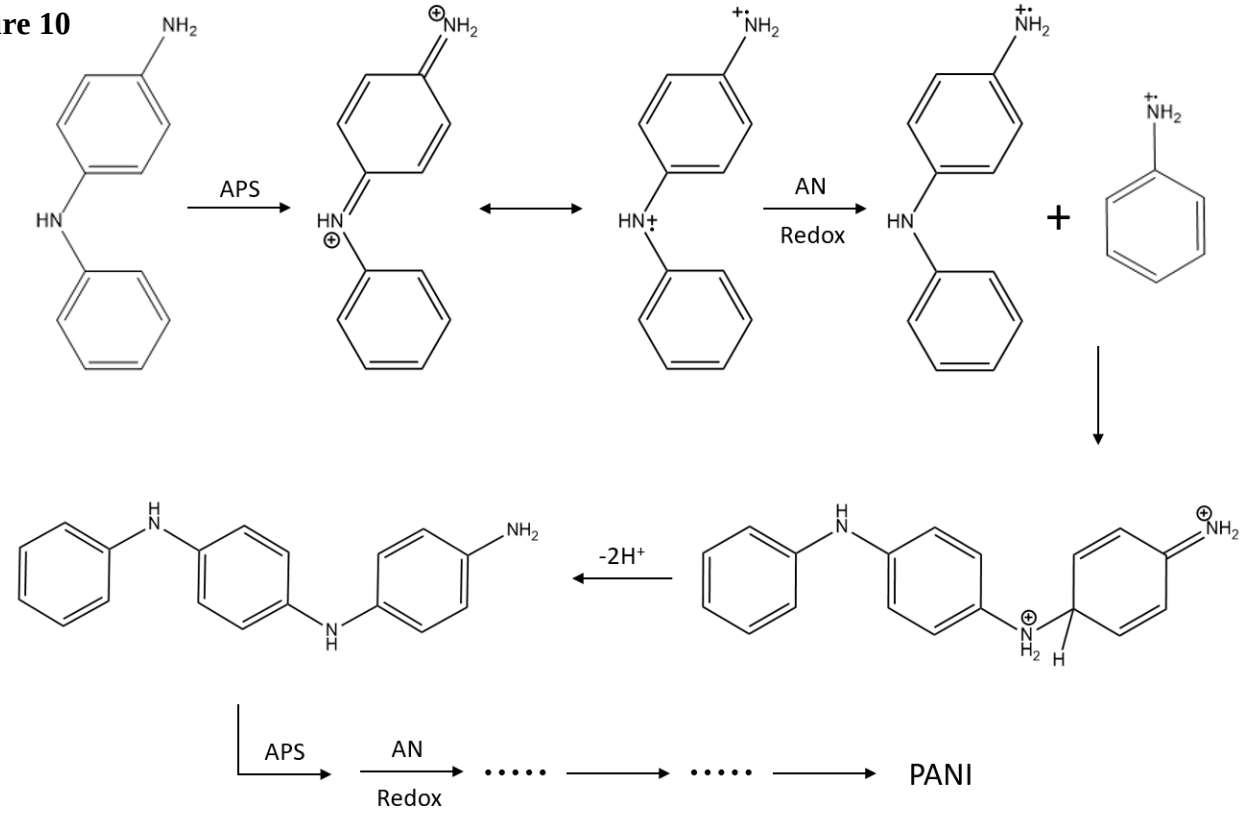

Figure 10. Mechanism for polyaniline propagation.

(OANI) and PANI, these chains are much more susceptible to oxidation by APS than AN since the chains will be more resonance stabilized [59]. Once oxidized to $[OANI]^{+2}$/$[PANI]^{+2}$, a redox reaction occurs with an unreacted aniline molecule resulting in $[OANI]^{\bullet+}$/$[PANI]^{\bullet+}$ and $AN^{\bullet+}$. At this point the two cationic radicals combine and the OANI/PANI chain propagates. This cationic radical mechanism for propagation was proven experimentally when it was seen that the reaction was greatly hindered by the presence of radical cation traps [60]. Computational studies were performed on OANI to see if propagation was possible by nitrenium cations. The calculations agreed with experimental studies that the radical cation mechanism was much more likely [61]. The reactions for the addition of the first aniline monomer to 4-ADPA can be seen in **Figure 10**. As with dimerization, the regioselectivity of this combination is dependent on the environmental

Figure 11

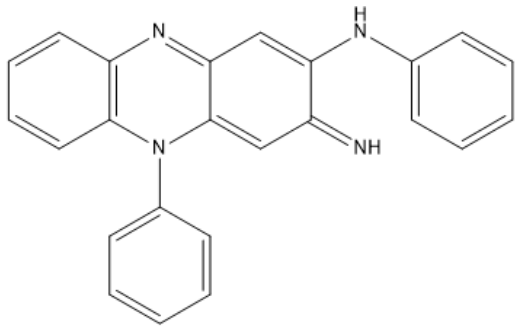

Figure 11. A possible aniline tetramer, one of many compounds which fall into the broad category "pseudo-mauveine," formed at a more basic pH.

conditions, particularly pH. It has been proven that at more basic pH the redox reaction between the growing OANI and an aniline molecule occurs less readily, instead performing a Michael addition on a non-terminal phenyl ring [62]. Further subsequent oxidation and aniline additions result in phenazine derivatives, also known as pseudo-mauveines a structure which can be seen in **Figure 11**. This matches well with experimental evidence for mauveine synthesis, first performed by Perkin over 150 years ago [63]. Mauveine was actually the first synthetic dye produced, first identified at "aniline purple" and later "Perkin's violet" [64].

Reaction Kinetics

Figure 12 shows standard curves used to determine the kinetics of PANI polymerization [65]. The curves clearly show a long initiation process with slow aniline consumption followed by a sharp increase in monomer conversion. This two-step kinetic curve is an excellent example of an autocatalytic reaction. Three steps of PANI polymerization mechanism have been discussed, initiation, dimerization, and propagation, as well as a side reaction of the propagation step resulting in aniline purple. Few kinetic studies have been performed which observe the rate of aniline initiation and dimerization independently, the two processes typically being as studied as a single initiation step. PANI polymerization kinetics are almost always studied by observing the

Figure 12

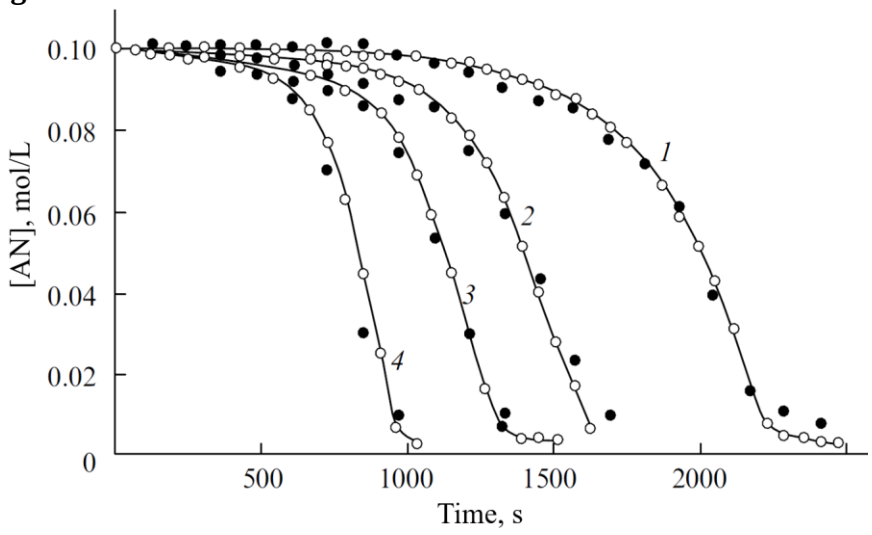

Figure 12 depicts typical kinetic curves of aniline polymerization. $[AN]_0$ = 0.10M, $[APS]_0$ = 0.125M. The reactions proceeded at: 1) 15°C, 2) 25°C, 3) 30°C, 4) 35°C. Data taken by potentiometry (○) and UV/Vis (●). Figure taken from Mezhuev *et al* [67].

rate of aniline consumption. By observing this variable alone, it is impossible to determine whether the products are PANI or pseudo-mauveine. While a seemingly enormous oversight, it is inconsequential from a synthetic standpoint since mauveine and its derivatives are very/slightly soluble in methanol/water respectively and are washed out in post-synthesis cleaning. Following these approximations, one can deduce the following kinetic expression from Wei *et al* [66]:

$$-\frac{d[AN]}{dt} = k_1[AN][APS] + k_2'[AN][PANI] \quad (1)$$

During the initiation phase of the reaction, the k_1 term dominates since no PANI has yet been formed. With the production of a small amount of PANI, the k_2 term quickly becomes dominant and PANI propagates rapidly. This kinetic expression is well agreed upon since it has been observed that the addition of pre-synthesized PANI to the system accelerates the reaction [22, 67]. Using equation 1 as a model for the polymerization, $k_1 = 4.18 \times 10^{-3}$ M^{-1} min^{-1} and $k_2 = 4.42$ M^{-1} min^{-1} at 4°C in 1 M HCl [22]. This difference of approximately 10^3 between k_1 and k_2 is fairly constant over a wide range of synthetic conditions.

Increased acidity has actually been shown to increase the reaction rate which is counterintuitive since H^+ is a product of the reaction [68]. Both k_1 and k_2 have been shown to exponentially increase with increasing acidity from [HCl] = 0.25 M to 1 M with k_1 increasing more rapidly [68]. This relationship has lead researchers to believe that there must be a proton transfer mechanism at work in the polymerization [22].

While this relationship between acidity and rate has been well documented, the effect of temperature on k_1 and k_2 is less quantified though it can easily be observed in **Figure 12** [65]. This temperature dependence on kinetics is the reason why some syntheses are performed at low temperatures. In order to increase the molecular weight of synthesized PANI one would need to maximize the ratio of k_2/k_1, essentially causing as few initiation events as possible so that aniline propagates into higher molecular weight chains. The enhanced performance of higher MW polymers is well documented and will be discussed in the subsequent section.

In addition to the autocatalytic nature of PANI, it has been observed that other materials will also accelerate the polymerization [22]. This kinetic variation is apparent in the curves shown in **Figure 13**. In order to account for the fact that the reaction is catalyzed by any surface, not PANI exclusively, the following equation was proposed by Tzou *et al* [22]:

$$-\frac{d[AN]}{dt} = k_1[AN][APS] + k_2\sigma[AN]S \qquad (2)$$

Figure 13

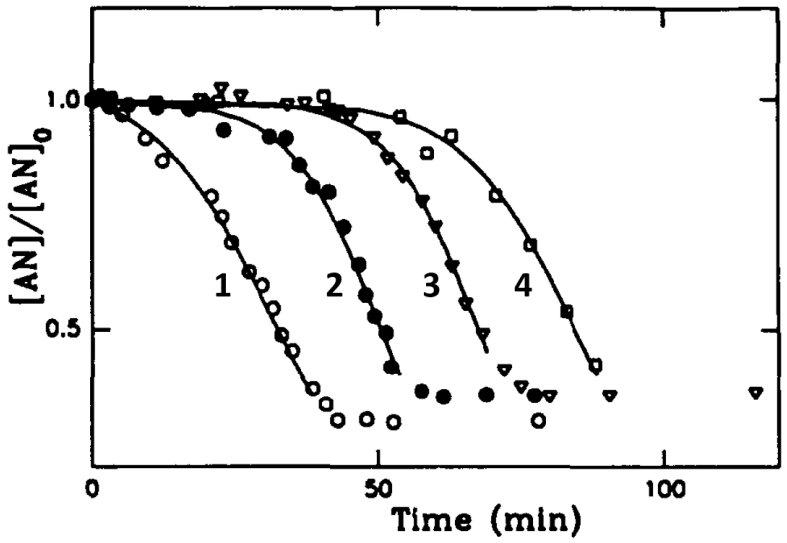

Figure 13. Polymerization kinetics in the presence of different surfaces: 1) PANI, 2) Al_2O_3, 3) clean fabric, 4) no substrate. Taken from Tzou *et al* [24].

This expression is similar to equation (1) except that the [PANI] term is replaced by the total surface area available (S) and the catalytic activity of the surface (σ). Since the catalytic activity is empirical and the interfacial area present in the system is determined by the amount of polymer formed, equations (1) and (2) are equivalent.

Effect of Chain Length on Polymer Properties

The simplest way to visualize polymers is as a collection of molecular ropes or chains with interactions of varying strength between individual chains. It is these intermolecular interactions which dictate the majority of observed properties of the polymer. It is obvious that longer polymer chains will have more opportunities for interactions with neighboring chains and, therefore, improved properties. One mechanical property which can be changed by varying chain length is the hardness of a material. An example of this was seen in a study by Al-Nasassrah *et al* where the tensile properties of various MW polyethylene glycols from 4,000 to 35,000 Da were determined [69]. The difference was evident with a five-fold increase in toughness

and over two-fold increase in stress required to fracture the material. Other mechanical properties can also be affected by a large distribution of molecular weights. The presence of very low weight oligomers or monomers which can act as an intermolecular lubricant, also known as a plasticizer, and soften the polymeric material [70].

Unlike other materials, polymers typically exist as a combination of crystalline and amorphous regions. Crystallinity is one of the most important properties to electrical conductivity in ICPs because it has been shown that charge carriers travel much more easily through crystalline regions [5]. One can imagine the ICP as conductive islands of crystalline material separated by amorphous areas with little conductivity. In this system conduction occurs when electrons tunnel between high conductivity islands. Higher MW polymers tend to exhibit higher degrees of crystallinity, though this trend does plateau. Researchers have tried numerous ways of increasing the crystallinity of PANI including spin-casting [71], stretch-alignment or "drawing" [72], and annealing [73] the films. In addition to increasing crystallinity, PANI/carbon nanotube composites have been fabricated in an attempt to bridge the amorphous regions with the conductive nanotubes [21, 74]. An excellent way to achieve a small distance between neighboring chains is by creating PANI with high degrees of crystallinity by synthesizing the polymer with a high MW.

Thermally Induced Crosslinking of PANI Backbones

While PANI in both the EB and ES states have been shown to be stable in air at ambient temperature, the dry polymer undergoes an irreversible transformation which occurs at elevated temperatures. This change has been identified as thermally-induced chemical crosslinking of the PANI backbones. It should be noted that other crosslinking reactions have been observed in

PANI including the chemical crosslinking caused by performing the synthesis in the presence of chemical crosslinkers [75] and solution-based physical crosslinking which occurs naturally over time [76]. For the purposes of this discussion, "crosslinking" will refer to thermally-induced chemical crosslinking unless otherwise specified. The structure of crosslinked PANI, shown in **Figure 14**, was proposed by Scherr *et al.* and involves the imine nitrogen forming a covalent bond with a quinoid ring of a neighboring chain resulting in the crosslinked network polymer [1]. The structure of crosslinked PANI has been verified spectrographically by observing the relative intensities of the quinoid and benzoid peaks via FTIR [77]. The change is also evident in solid state C^{13}NMR by the decreased intensity of the imine carbon peak accompanied by the increased intensity of the non-protonated carbon peak [78]. The kinetics of the crosslinking reaction have

Figure 14

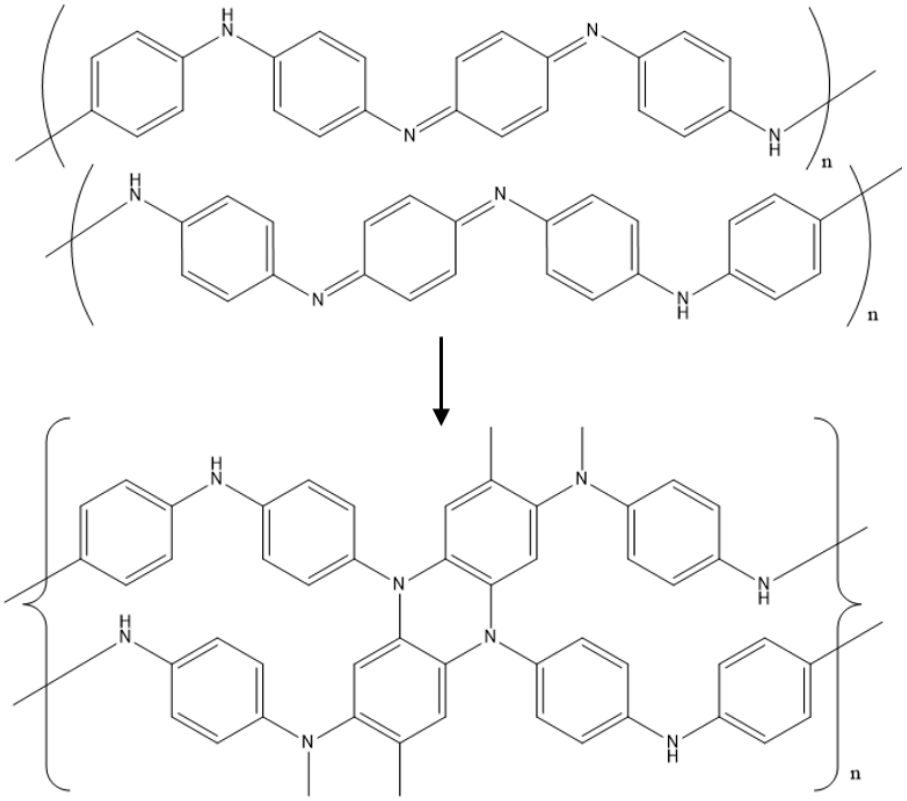

Figure 14. Structure of crosslinking PANI first proposed by Scherr *et al.* [1] and in agreement with several investigative methods such as FTIR [77] and NMR [78].

been studied using DSC by Luo *et al.*[79] Luo performed two analytical methods [80-81] to determine that the activation energy of the crosslinking reaction was 111 kJ/mol. While the final structure of thermally crosslinked PANI is well agreed upon, the mechanism behind the process is still debated.

Crosslinked PANI behaves differently from its un-crosslinked predecessor is several ways, most of which are undesirable. Due to crosslinking, the PANI chains are more tightly bound together which makes introducing other species into the solid polymer more difficult. As a result, crosslinked PANI is much less soluble in NMP since the solvent can no longer separate the polymer chains. Another effect of the tightly bound chains is that the films can be doped less thoroughly upon acid treatment [82]. As a direct result of this doping difficulty, the conductivity of crosslinked films decreases by several orders of magnitude even when the film is reintroduced to a solution of the dopant [83]. One positive effect of crosslinking is that the mechanical properties of PANI films improves with increasing temperature, a trend that continues until the polymer begins to degrade at higher temperatures [82].

Surface Features of PANI Films

One aspect of PANI which has been under examination recently is the supramolecular structures the polymer formed when synthesized under varying conditions [84]. For example when polyaniline is synthesized in solution with sunset yellow dye it forms choral-like structures with enhanced conductivity [85], in a solution of 0.4 M acetic acid it forms nanotubes [86], and in a solution of ammonia it forms microspheres [86]. While these high surface area structures may be useful for energy storage purposes such as supercapacitors [87-88] and batteries [89], many applications for PANI films involve the charge transport from the polymeric film to a conductor

or other semiconductor. A few devices which would require this heterojunction between an ICP and neighboring material are solar cells and field effect transistors. High voltages are typically needed for ICP based electrical devices due to the poor charge transport between the polymer and the metal electrode [90]. This difficulty in charge transport is likely due to very small peaks in the surface of the polymer resulting in only a small area of the surface in contact with the surface of the metal [90].

CHAPTER 3
OBJECTIVE

In order for a material to reach its full potential, every aspect of its production must be scrutinized for optimization. Means of controlling intrinsic properties of the material are important, particularly with widely used materials like ICPs. Two aspects of PANI synthesis will be varied in order to determine their effect:

1. Synthesis temperature of aniline polymerization
2. Post-synthesis soxhlet extraction

The objective of this research is to determine how these two characteristics of the PANI production process change the properties of their cast films, specifically properties which have been shown to affect the electrical conductivity of the PANI films.

CHAPTER 4
EXPERIMENTAL

Synthesis of Polyaniline

Polyaniline was synthesized as emeraldine salt via polymerization with APS as the oxidizer and HCl as the dopant. Aniline was first dissolved in 1 M HCl or 1 M HCl/4 M LiCl if the synthesis was to be carried out below 0°C. Synthesis carried out at 0°C were performed in a standard ice bath. Syntheses done below 0°C were performed in a bath of water/ethylene glycol and held at a constant temperature by an immersion cooler. A 1 M APS solution was prepared by dissolving the APS in a 1.2:1 mole ratio to the aniline. The APS solution was made in 1 M HCl or 1 M HCl/4 M LiCl depending on reaction temperature. The APS solution was added dropwise to aniline solution at a rate of 2 mL/min. The reaction was allowed to stir at least 24 hours after the addition of the APS. The dark green solution was then filtered using standard vacuum filtration and the ES collected. The ES was allowed to dry at 50°C for 2 hours before being added to a solution of 1 M NH_4OH. The solution was stirred overnight in order to allow the ES to dedope forming EB. The EB was then filtered and the resulting dark blue powder was dried at 50°C overnight. Half of the resulting EB was stored in a glass vial under nitrogen atmosphere for later analysis. A soxhlet extraction was performed on the remaining EB. Methanol was used as the solvent and was replaced as needed. The soxhlet extraction proceeded until the solvent ran clear, typically 7 days. Upon completing the extraction, the EB was dried at 50°C and stored in the same manner as the un-extracted EB. A flow chart of this synthesis is provided in **Figure 15**.

Figure 15

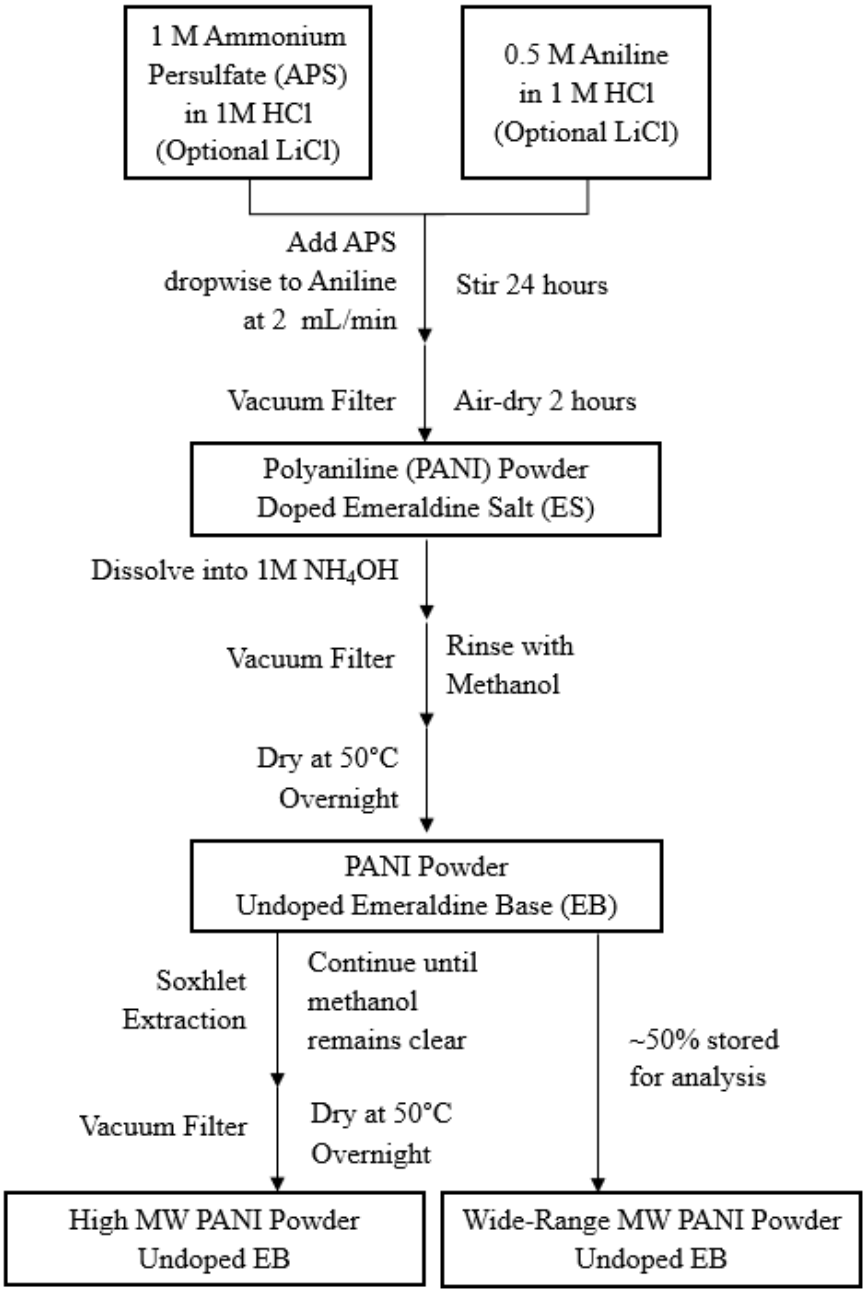

Figure 15. Steps for the synthesis of PANI ES and its subsequent dedoping to EB and extraction to increase molecular weight.

Film Preparation

Films were cast using NMP or DMPU as a solvent. A 5% weight solution of PANI was made by slowly adding solid EB to stirring containers of solvent over six to eight hours. It was observed that films cast from these solutions looked as if there were undissolved particles which could not be filtered out of solution by vacuum filtration. In order to remove these particles, the PANI solution was centrifuged for 15 minutes at 3000 rpm. The centrifugation resulted in a clay-like solid bottom layer and a liquid top layer. The bottom layer did not form films and was discarded. The top layer was pipetted into a petri dish and the solvent evaporated off at 50°C, a process which typically took several days. The EB film was then doped back to ES by the addition of 1 M trifluoromethanesulfonic acid (CF_3HSO_3) to the petri dish and soaking for 6 hours. In addition to doping the PANI films, the overnight soak in acid caused the films to come free from the petri dishes. The films were then air-dried for an hour and their conductivities measured. A flow chart of the steps for film preparation has been provided in **Figure 16**.

Characterization

The EB powder was characterized for functionality by a Bruker Optics Alpha FTIR with an attenuated total reflectance diamond cell. Thermogravimetric analysis was performed using a TA Instruments model Q-5000 TGA. Differential scanning calorimetry was performed using a TA Instruments model Q-2000 DSC. The temperature of the DSC was increased by 2°C/min up to 350°C and was performed under a nitrogen blanket flowing at 5 ml/min. Gel permeation chromatography was performed by the Georgia Tech Research Institute. GPC was performed on a Waters 600 HPLC using a HSPEG2 column. The mobile phase was THF and the standards were poly (2-vinylpyridine) with a molecular weight range from 35 – 240 KDa. Degree of

crystallinity was determined by X-ray diffraction on a Rigaku MiniFlex II Benchtop X-Ray Diffractometer. Electrical conductivity was determined using a Jandel RM3-AR four-point probe. Conductivity was determined using a current of 100 mA. At least ten conductivity measurements were taken on each sample in order to account for variation of the samples surfaces'. Samples were photographed in order to observe surface roughness.

Figure 16

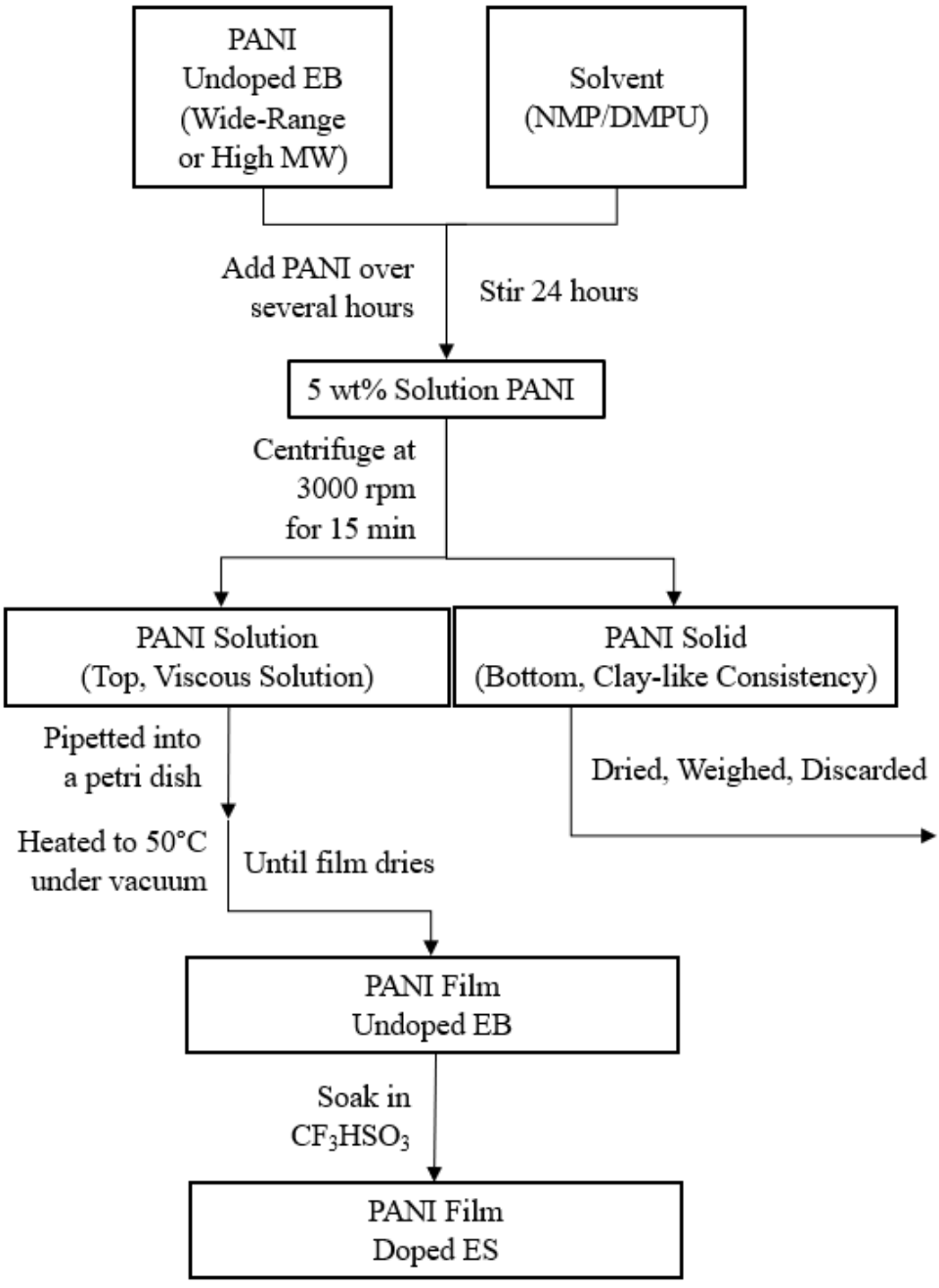

Figure 16. Steps for Preparing EB films and its subsequent doping to ES.

CHAPTER 5

RESULTS AND DISCUSSION

X-Ray Diffraction

X-ray diffraction (XRD) was performed in order to determine the crystallinity of EB powders. An increase in crystallinity would result in improved electrical conductivity since the high crystallinity would indicate a predisposition for the polymer to exist in an ordered state. **Figure 17** compares the XRD patterns of the two samples prepared at -10°C with one sample having undergone a soxhlet extraction while the other did not. One important aspect of these patterns which must be addressed is the very broad "peak" around 21 2θ, an artifact called the amorphous halo. While most peaks in an XRD pattern are the result of some form of order in the material, the amorphous halo is formed due to the random orientation of polymer chains [91]. This random orientation causes random scattering of the radiation resulting in a peak that is relatively broad compared to peaks caused by crystallinity. Comparing the extracted and unextracted PANI in **Figure 17**, it appears as if the amorphous halo gets larger compared to the peak at 25 2θ. This trend was observed in XRD patterns for all samples. This peak at 25 2θ is usually associated with doped ES, the XRD pattern of ES usually having only the single amorphous peak [92-93]. The presence of the 25 2θ peak indicative of doped ES suggests that the PANI sample was not completely dedoped by the NH_4OH solution. The reduction of this peak relative to the amorphous halo by the soxhlet extraction suggests that the extraction removes some of the dopant.

A comparison of EB synthesized at different temperatures can be seen in **Figure 18**. It can be seen that the cold-temperature syntheses are significantly more crystalline than the room temperature synthesis, though this trend does not seem to continue between the sub-0°C

syntheses. The room temperature synthesis is obviously less crystalline due to the significant presence of the amorphous halo around 20 2θ. The other unique aspect of the room temperature synthesis PANI is the peak at 6 2θ. This peak has not yet been identified though it has been observed by other researchers [94].

The post-synthesis heating also did not affect crystallinity, evident in **Figure 19**. The sample in **Figure 19** was dried under a lamp at room temperature in order to avoid heating the powder before XRD was performed. The XRD patterns are taken from the same sample which was heated to 67°C and then 100°C for several hours before the respective XRD analysis. The height of the peak at 21 2θ does not increase relative to the amorphous halo, indicating no change in crystallinity. While most polymers can be made more crystalline by holding the material at elevated temperatures, several studies indicate that this is rarely the case for EB[73, 95].

Figure 17

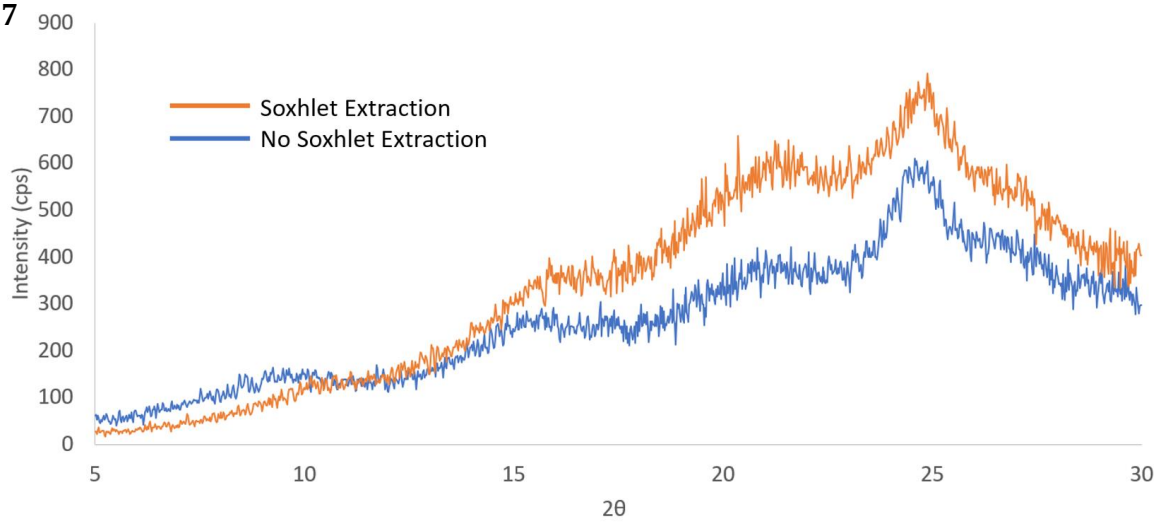

Figure 17. Comparison of the XRD pattern of EB powder made in the same synthesis at -10°C with one sample having undergone a soxhlet extraction and the other being analyzed as-synthesized. The XRD data suggests an increase in crystallinity as a result of the soxhlet extraction.

Figure 18

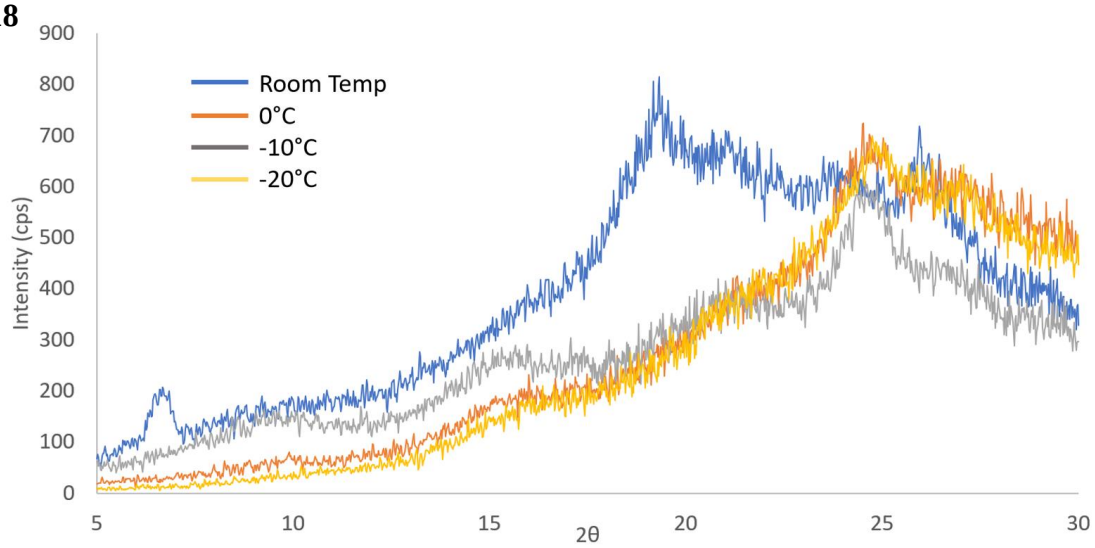

Figure 18. Comparison of the XRD pattern of EB powder synthesized under a variety of temperature conditions and not having undergone a soxhlet extraction. This comparison shows a large decrease in the amorphous halo between the room temperature synthesis and the 0°C synthesis. This data presents no clear correlation between synthesis temperature and crystallinity for PANI synthesized temperatures below 0°C. The peak at 6 2θ on the Room Temp diffraction data has not been identified but has been observed by other researchers [94].

Figure 19

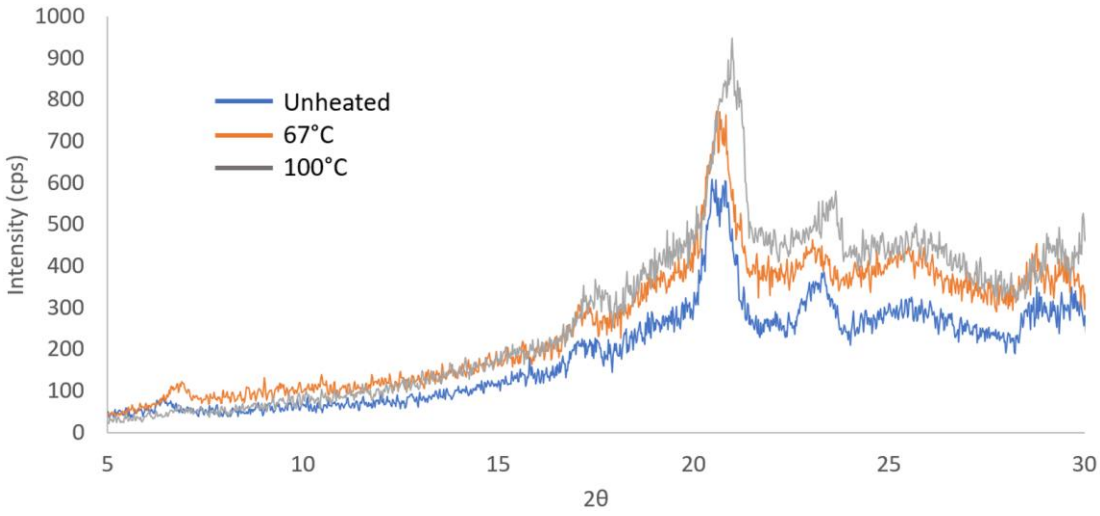

Figure 19. Comparison of the changes in XRD patterns of a single sample of EB as it is heated. The relative height of the 21 2θ peak does not change indicating no change in crystallinity.

Gel Permeation Chromatography

Gel Permeation chromatography was performed on select samples in order to determine the relative molecular weight of the PANI. A comparison of the relative molecular weight and polydispersity index can be seen in **Table 1**. By comparing the synthesis temperatures, it can be seen that the decreased temperature does result in polymer chains of higher molecular weight. This data suggests that decreased synthesis temperature may decrease the kinetics of aniline initiation more heavily than polyaniline propagation, resulting in fewer initiation events which results in fewer, longer PANI chains.

This GPC data also sheds light on another aspect of the of this synthetic method; the result of the soxhlet extraction. The soxhlet extraction increased the average molecular weight of PANI synthesized as both room temperature and -20°C by 4.7% and 8.2% respectively. The effect of the soxhlet extraction is also evident from the change in polydispersity index (PDI). The

Table 1

Synthesis Temperature	Soxhlet Extraction	Average Molecular Weight (M_N)	Polydispersity Index
Room Temp	No	37,600 Da	3.2
Room Temp	Yes	39,400 Da	2.6
0°C	No	44,200 Da	3.0
-20°C	No	52,400 Da	3.4
-20°C	Yes	56,700 Da	2.4

Table 1. Comparison of the number average molecular weight and polydispersity index of various samples.

increase in molecular weight and decrease in PDI indicates that the low molecular weight PANI and OANI chains were removed from the sample during the soxhlet extraction.

Electrical Conductivity

Measurements of the electrical conductivity of the cast PANI films was performed with the Jandel four-point probe. In this measurement, current is applied to a pair of probes and the voltage drop is measured by two different probes which are in line between the current probes. A four-point probe is advantageous for conductivity measurements of semiconductors because, if only two paints are used for simultaneous charge injections and voltage measurement, charge injection discrepancies can occur at the probe-material interface and affect the measured voltage drop. These injection discrepancies are significantly decreased if the current is supplied between a different pair of probes than the probes measuring the voltage drop.

Table 2

	-20°C No Soxhlet	**-20°C Soxhlet**	**-20°C No Soxhlet**	**-20°C Soxhlet**
Solvent	NMP	NMP	DMPU	DMPU
Average Resistivity	940.97 mΩ/□	835.25 mΩ/□	814.22 mΩ/□	572.10 mΩ/□
Standard Deviation	222.91 mΩ/□	152.85 mΩ/□	183.55 mΩ/□	50.40 mΩ/□
% Deviation	23.69 %	18.30%	22.54%	8.80%

Table 2. Comparison of the conductivity of samples synthesized at -20°C. It can be seen that samples which have undergone an extraction have less resistance. It can also be seen that films made from casting with DMPU are less resistive than films cast with NMP.

The effect of soxhlet extraction on electrical conductivity can be seen in **Table 2**. The difference in conductivity between PANI subjected to a soxhlet extraction and PANI that had not is evident in both samples cast in NMP and DMPU. The samples cast in NMP had a difference of 105 mΩ/□, which is within the standard deviation. The conductivity of the PANI samples cast from DMPU had less deviation and shows that a soxhlet extraction does increase the conductivity of PANI films.

The effect of synthesis temperature on electrical conductivity can be seen in **Table 3**. While one may be able to extrapolate the trend of increasing resistivity with increasing synthesis temperature, the large deviation of samples of higher synthesis temperature makes it unclear. The large deviation is most likely due to the lack of mechanical integrity of the sample. Films cast from PANI synthesized at room temperature and 0°C were much more brittle and, while being doped in the triflic acid, began to break apart. An easily audible crunching sound could be heard when the four-point probe was lowered onto contact with these brittle samples while no noise

Table 3

Synthesis Temperature	Room Temperature	0°C	-10°C	-20°C
Average Resistivity	2330 mΩ/□	1130 mΩ/□	332.07 mΩ/□	799.24 mΩ/□
Standard Deviation	1238 mΩ/□	244.96 mΩ/□	121.44 mΩ/□	71.34 mΩ/□
% Deviation	53.13%	21.68%	36.57%	8.93%

Table 3. Comparison of the conductivity of samples synthesized at various temperatures. While a trend for increasing conductivity with increasing molecular weight can be seen, the data is inconclusive due to large standard deviation.

could be heard from the films from -10°C and -20°C synthesis. The mechanical failure of the brittle samples can be seen in the pictures of the samples in subsequent sections.

Thermal Analysis

TGA and DSC were performed on the EB powder samples in order to determine whether the synthesis temperature or soxhlet extraction had any effect on the thermal properties of the PANI. A typical overlay of these two analyses can be seen in **Figure 20.** Three thermal events can be seen using these techniques: one from the starting temperature to 150 °C, a second from approximately 225°C to 300°C, and a third occurring above 300°C. The first event can be seen in the TGA as a loss of approximately 4-10% weight loss accompanied by a broad endotherm in the

Figure 20

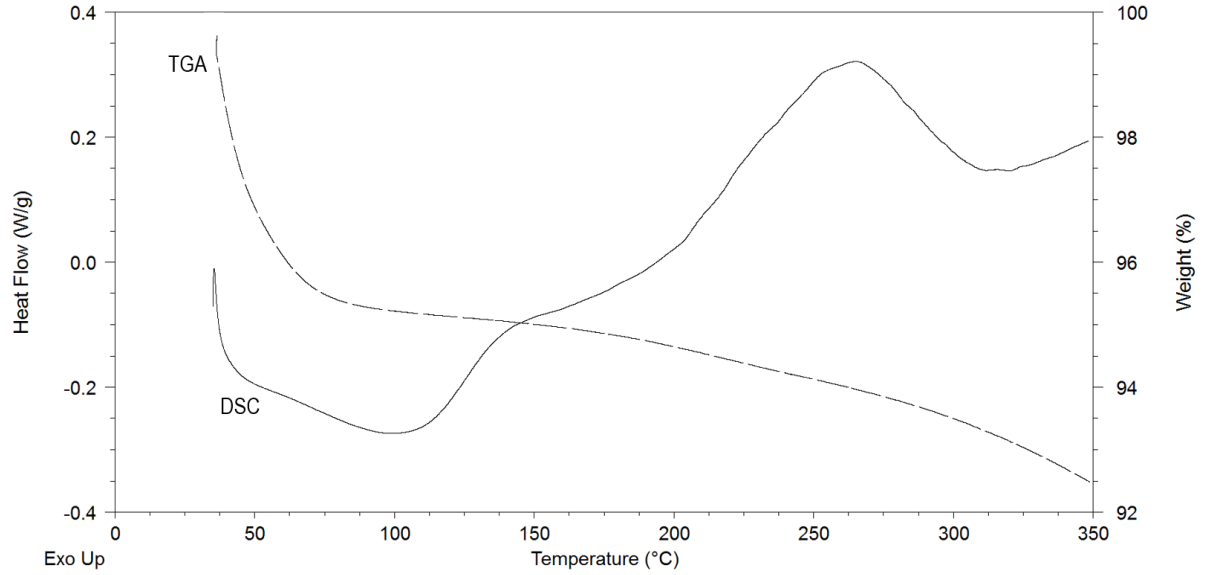

Figure 20. A typical example of TGA and DSC data. This data was taken of EB samples synthesized and soxhlet extracted simultaneously. The synthesis was performed at 0°C. This graph was produced with TA Universal Analysis data processing software.

DSC. This first event is attributed to a loss of dopant and residual solvent which remains even after drying the powder. It should be noted that the temperature at which the dopant is lost is very dependent on the dopant's structure. For example a structurally small and simple dopant such as HCl is lost before 100°C [83] while large, bulky dopants such as 4-dodecylbenzenesulfonic acid have been shown to remain trapped in the polymer until 250°C [96]. This solvent/dopant peak is not seen again when the same sample is heated a second time which means that this peak cannot be attributed to a reversible thermal transition of the polymer such as a glass transition point. The second event can be seen as a very small weight loss in the TGA accompanied by a broad exotherm in the DSC from approximately 225°C to 300°C. This has been attributed to crosslinking of the polymer backbone. The third event is a continual decrease in weight on the TGA accompanied by an increasing exotherm on the DSC above 300°C. This event is the thermal degradation of the polymer, reducing the polymer to ash.

Two distinct differences can be observed from the thermal analysis in this study. The first difference is between extracted and unextracted samples and deals with the solvent lost before 150°C. This difference is visible in both TGA and DSC analyses, **Figure 21** and **Figure 22** respectively. The difference in weight loss below 150°C between extracted and unextracted samples is evident in the TGA shown in **Figure 21.** The extracted samples lost an average of 5.01% mass and the unextracted samples lost an average of 10.46% mass. This difference is also noticeable in **Figure 22** which compares the DSC of extracted and unextracted EB synthesized at -20°C. The smaller endotherm in the extracted sample indicates that there is less solvent being heated from the sample, which is in agreement with the TGA data. Samples which have not been soxhlet extracted come into contact with water as a solvent almost exclusively before being dried and analyzed. On the other hand, soxhlet extracted samples spend approximately a week being

washed with methanol before drying and analysis. With previous solvent exposure and thermal analysis, it can be concluded the PANI has a higher affinity for water than for methanol.

The second noticeable difference from the thermal analysis is the size of the exotherm between 150°C and 275°C which has been shown to be associated with PANI crosslinking. A soxhlet extraction causes the crosslinking exotherm to increase in size and for the maxima to shift toward a higher temperature. This phenomenon is most easily observed in a comparison of DSC data, shown in **Figure 22**. This trend can also be seen comparing the DSC of EB synthesized at different temperatures, seen in **Figure 23** and calculated in **Table 4**. This data suggests that PANI chains of higher molecular weight crosslink less readily compared to lower molecular weight chains. The dependence of crosslinking rate on molecular weight has actually been observed before, though it was not attributed to crosslinking at the time [97]. Interestingly, the opposite trend was observed for solution-based crosslinking by Oh *et al*. who reported that solutions of higher molecular weight PANI in NMP crosslinked faster than solutions made from low molecular weight PANI [76, 98].

Figure 21

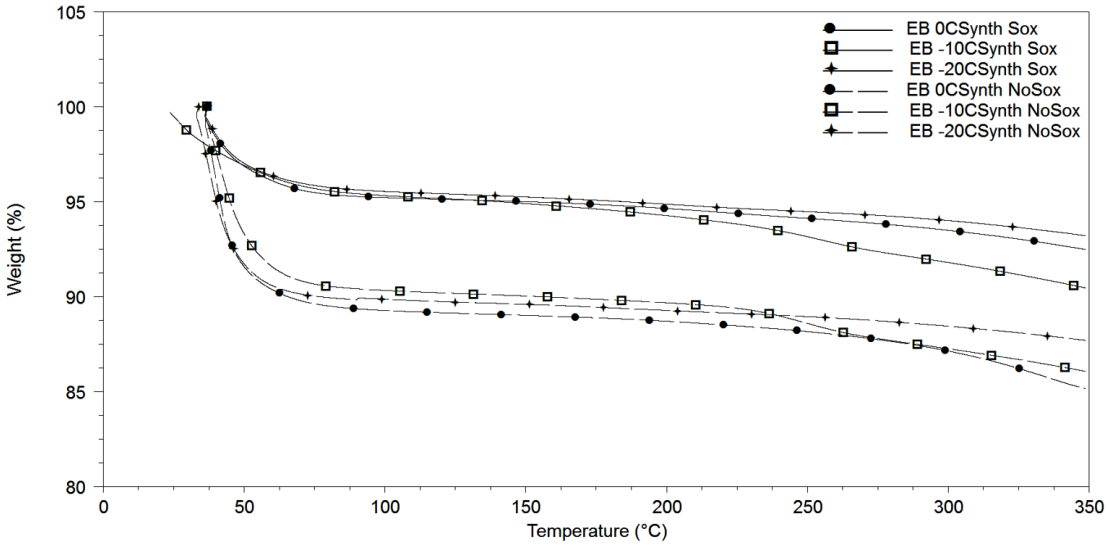

Figure 21. An overlay of all TGA data from sub-zero synthesis. Samples that have undergone a soxhlet extraction are depicted with solid lines while sample that have not undergone extraction are depicted with dashed lines. It is evident that unextracted samples lose much more solvent from the larger weight loss below 100°C. This graph was produced with TA Universal Analysis data processing software.

Figure 22

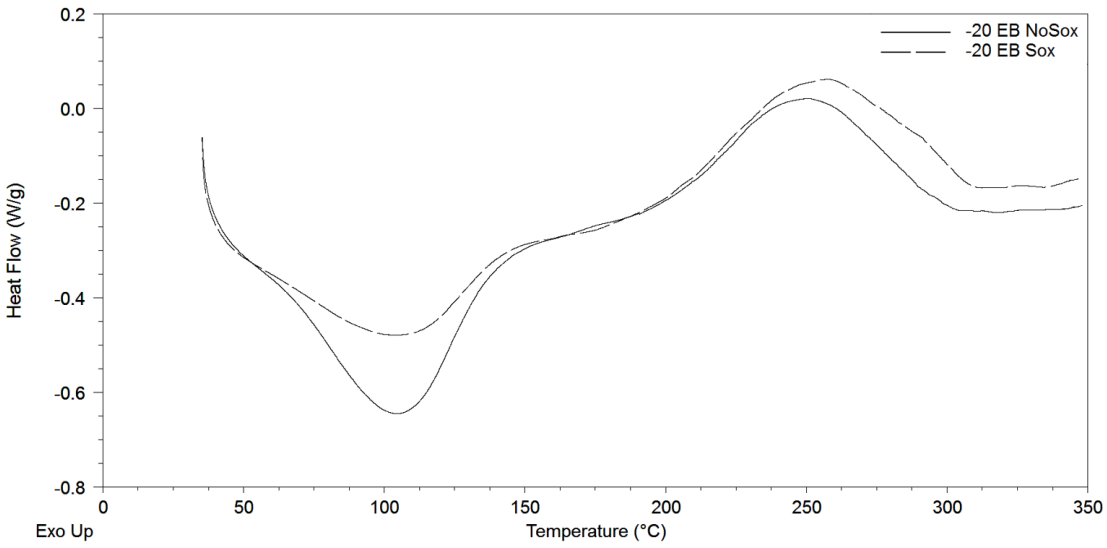

Figure 22. A comparison of DSC data of extracted and unextracted EB synthesized at -20°C. The difference in both the solvent loss peak around 100°C and the crosslinking peak around 250°C are representative of samples synthesized at sub-zero temperatures. This graph was produced with TA Universal Analysis data processing software.

Figure 23

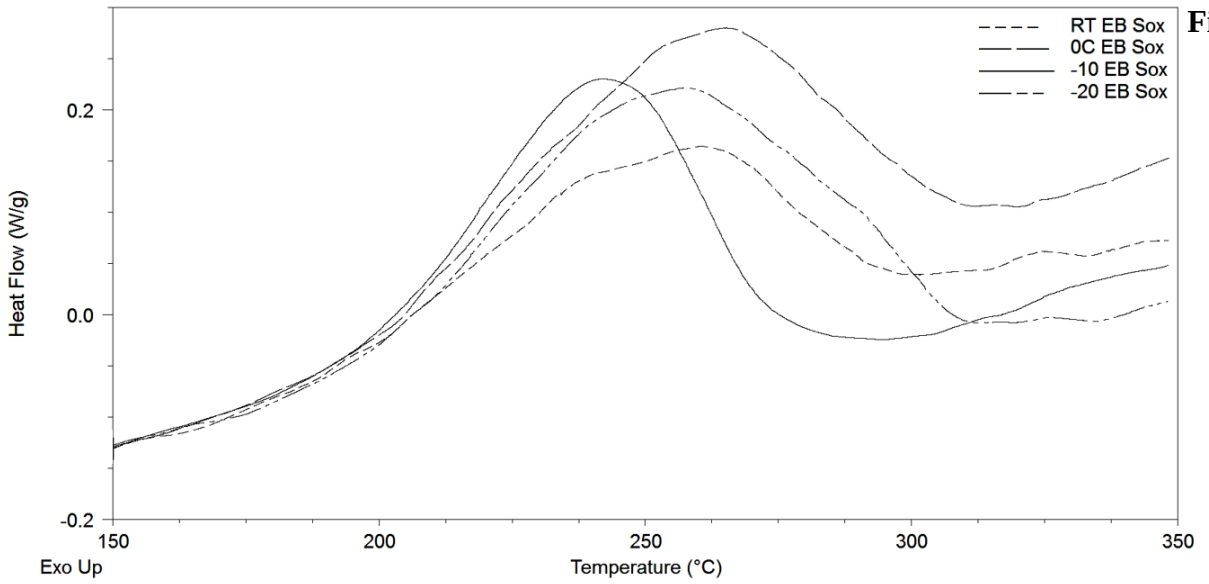

Figure 23. Comparison of the crosslinking peak of EB synthesized at different temperatures, all of which have been soxhlet extracted. The y-axis of the data has been shifted so that all curves are approximately equal from 150°C to 200°C. Because the integral is calculated with a sloping baseline, this shift does not affect the value of the integral. This graph was produced with TA Universal Analysis data processing software.

Table 4

Synthesis Temperature	Integral
Room Temp	122.2 J/g
0°C	184.4 J/g
-10°C	152.9 J/g
-20°C	207.9 J/g

Table 4. Integral of the crosslinking peak for each of the soxhlet extracted samples shown in **Figure 23**. The values are baseline-corrected integrals calculated by TA Universal Analysis data processing software. The integrals are calculated from 187.5°C to their local minimum. The only data point which does not fit a linear trend is from EB synthesized at -10°C which can be explained by the abnormally narrow peak width. The DSC of unextracted EB synthesized at -10°C also has an uncharacteristically narrow crosslinking peak and the two do follow the trend described above and seen in **Figure 22**.

In more thermodynamically appropriate terms, this peak shift indicates a positive correlation between chain length and activation energy (E_a) as well as total change in enthalpy (ΔH) of the crosslinking reaction, shown by a shift of the exotherm toward higher temperatures and an increase in the area of the exotherm respectively. One explanation for this difference in E_a and ΔH is that it may be due to variation in the mechanism of crosslinking between different portions of the polymer chain. For example, the reaction between a terminal nitrogen/phenyl ring and a section within the polymer backbone would differ thermodynamically from a reaction between two non-terminal portions of the PANI chain. Longer polymer chains have less terminal groups per gram which this data shows results in crosslinking reactions of higher E_a and ΔH.

Qualitative Film Properties

A reoccurring problem in film synthesis was the mechanical failure of films. Low molecular weight films synthesized at higher temperatures had a tendency to crack when soaked in aqueous medium. The extent of fracturing varied significantly. In some instances, fracturing resulted in pieces that were too small to retain their structure and curled in on themselves upon evaporation of the water as in **Figure 24A**. Samples with this mechanical frailty could not be tested for electrical conductivity. In later samples the fracturing was less extinctive, the films retaining their integrity enough for its conductivity to be tested as seen in **Figure 24C** and **Figure 24D**. A comparison between films of different synthesis temperatures can also be seen in **Figure 24C-F**. It is evident that higher molecular weight films are less susceptible to fracture than lower molecular weight films. It was also seen that low MW films cast with DMPU as the solvent do not fracture as easily as the films cast with NMP, evident when comparing room temperature synthesis films in **Figure 24C** and **Figure 24G**.

A reoccurring problem researchers face when working with polyaniline is crosslinking in solution which occurs slowly at room temperature. This crosslinking results in a gel which does not dry into a flat surface, but instead shrinks in on itself to form a very rigid bowl structure, seen in **Figure 24B**. As with heat-induced crosslinking discussed in the previous section, solution-based crosslinking has been observed by many researchers, but few studies exist focusing on the phenomenon.

Most electrical applications of polyaniline require the material to transport current from the PANI surface to another conductive surface. To do this efficiently, the surface of the PANI film should be as flat as possible in order to increase surface area in contact with the neighboring material. The fabricated films were observed under high magnification to determine surface roughness. Some of these images can be seen in **Figure 25.** It is evident that before being used in electrical applications a surface flattening procedure would need to be developed.

Figure 24

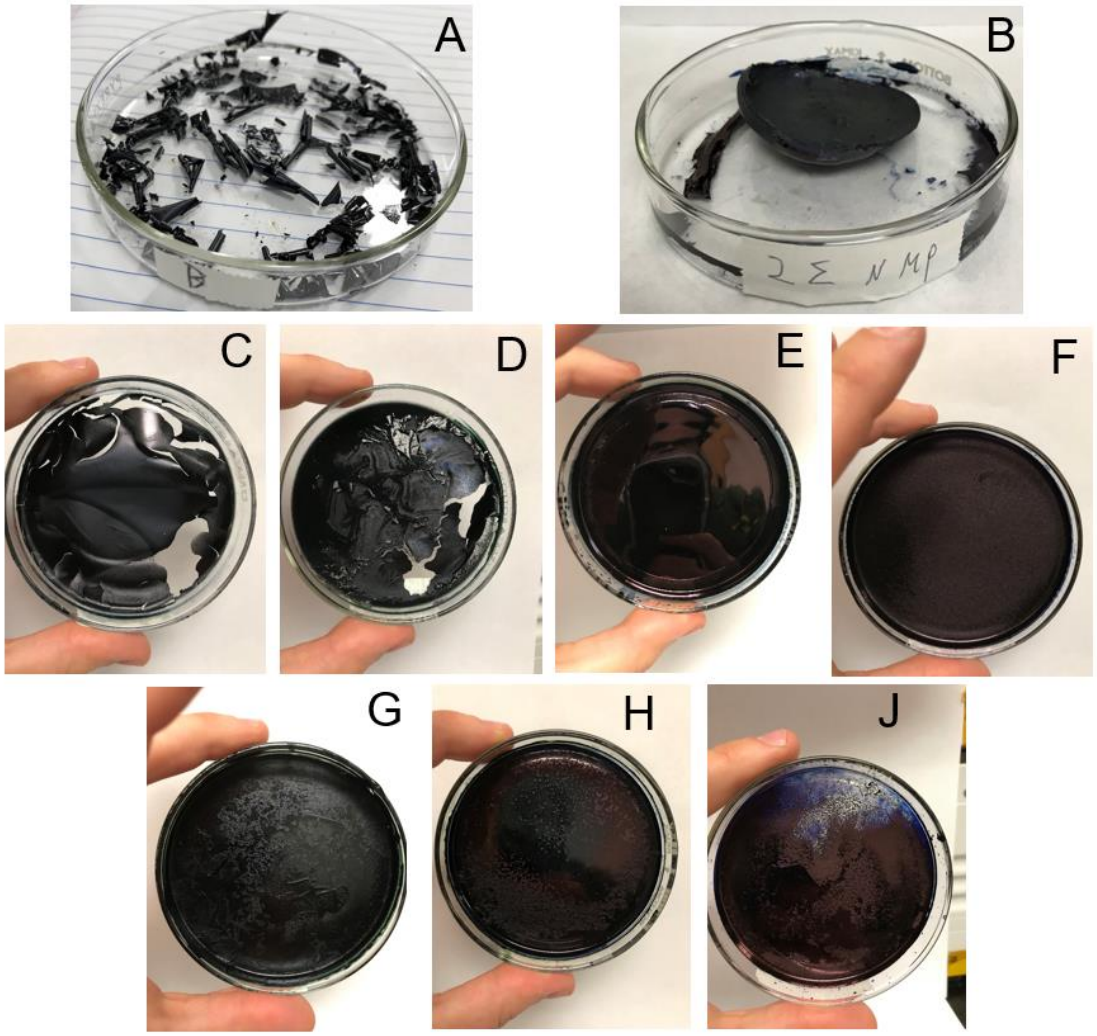

Figure 24. A collection of optical images of PANI films. The films are all in petri dishes 3 inches in diameter.

A) PANI film made from sample synthesized at room temperature which fractured when soaked in aqueous medium.

B) PANI film made from EB synthesized at room temperature and soxhlet extracted. The PANI/NMP solution gelled and dried into the bowl-shape shown.

C-J are most easily distinguished using the following table:

Figure 24	Synthesis temperature	Soxhlet Extracted	Solvent
C	Room Temp	No	NMP
D	0°C	No	NMP
E	-10°C	No	NMP
F	-20°C	No	NMP
G	Room Temp	No	DMPU
H	-10°C	No	DMPU
J	-20	Yes	NMP

Figure 25

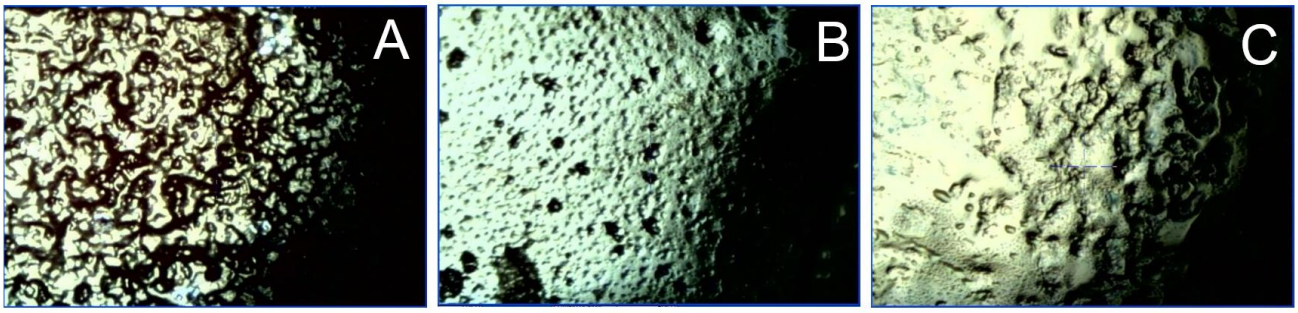

Figure 25. Zoomed optical images of PANI films. The images are of an area 520μm x 375μm.
A) EB synthesized at 0°C, not soxhlet extracted, cast with a solution of NMP.
B) EB synthesized at -20°C, soxhlet extracted, cast with a solution of DMPU.
C) EB synthesized at -20°C, not soxhlet extracted, cast with a solution of NMP.

FTIR

FTIR was performed to determine if either synthesis temperature or soxhlet extraction had any effect on the vibrational modes of the EB powder. Any change in these vibrational modes would indicate variations in the functional groups of the PANI powder samples. **Figure 26** shows the FTIR spectra of two samples synthesized together at -10°C to show the effect of soxhlet extraction. Characteristic peak determinations are in **Table 5** with assignments taken from Tang *et al* [99]. Three differences can be observed between extracted and unextracted samples: one in the relative intensities of the 1500 cm^{-1} and 1580 cm^{-1} peaks, a second in the shape of the peak around 1150 cm^{-1}, and a third in the peak(s) around 820 cm^{-1}.

The first difference between extracted and unextracted samples is the decreased ratio of the 1500/1580 cm^{-1} peaks of extracted samples. These peaks indicate the presence of benzoids and quinoids respectively. On average, the soxhlet extraction caused a 6% decrease in the benzoid peak compared to the quinoid peak. It has been shown that increasing presence of

dopant in ES results in increased absorption of the benzoid peak at 1500 cm^{-1} with the most heavily doped samples having a 1500/1580 cm^{-1} peak ratio of nearly 200% [99]. This increased benzoid presence indicates that the dedoping process with NH_4OH was insufficient to completely remove the chloride from the system, but that dopant removal was furthered or completed by the soxhlet extraction.

The second difference is an apparent narrowing and shifting of the peak centered around 1150 cm^{-1} when the EB undergoes a soxhlet extraction. The absorbance in this area is actually due to two different peaks, a narrow peak at 1160 cm^{-1} and a broad peak at 1140 cm^{-1}. When PANI was first being investigated by MacDiarmid, the 1160 cm^{-1} peak was referred to as the "electron-like band" [100] and was associated with the degree of electron delocalization and therefore electrical conductivity. Upon future investigation, it was seen that this peak was not growing with increasing dopant level and conductivity, but instead a new peak at 1140 cm^{-1} was appearing which is much stronger and broader than the neighboring peak at 1160 cm^{-1}. This 1140 cm^{-1} peak increases rapidly with increasing dopant level and drowns out the 1160 cm^{-1} peak with very little added dopant. It can be seen in **Figure 26** that unextracted EB has the broad 1140 cm^{-1} peak as well as the 1160 cm^{-1} peak, distinguishable as a shoulder. EB subjected to a soxhlet extraction had no evidence of this peak. This reinforces the conclusion that the dedoping with NH_4OH was incomplete and that the extraction removed some of the residual dopant.

The third difference is in the peaks centered around 820 cm^{-1} corresponding to the aromatic C-H out of plane bend. This artifact tends to be a single peak for samples which have been soxhlet extracted. Samples which have not been soxhlet extracted have the same peak at 820 cm^{-1} with an additional peak at 795 cm^{-1}. While this pair of peaks can be seen in many studies [101-103], to this researcher's knowledge it has never been commented on. This additional

peak is likely due to the incomplete dedoping, similar to the increased ratio of the 1500/1580 peaks and appearance of the 1140 cm^{-1} peak.

Figure 26

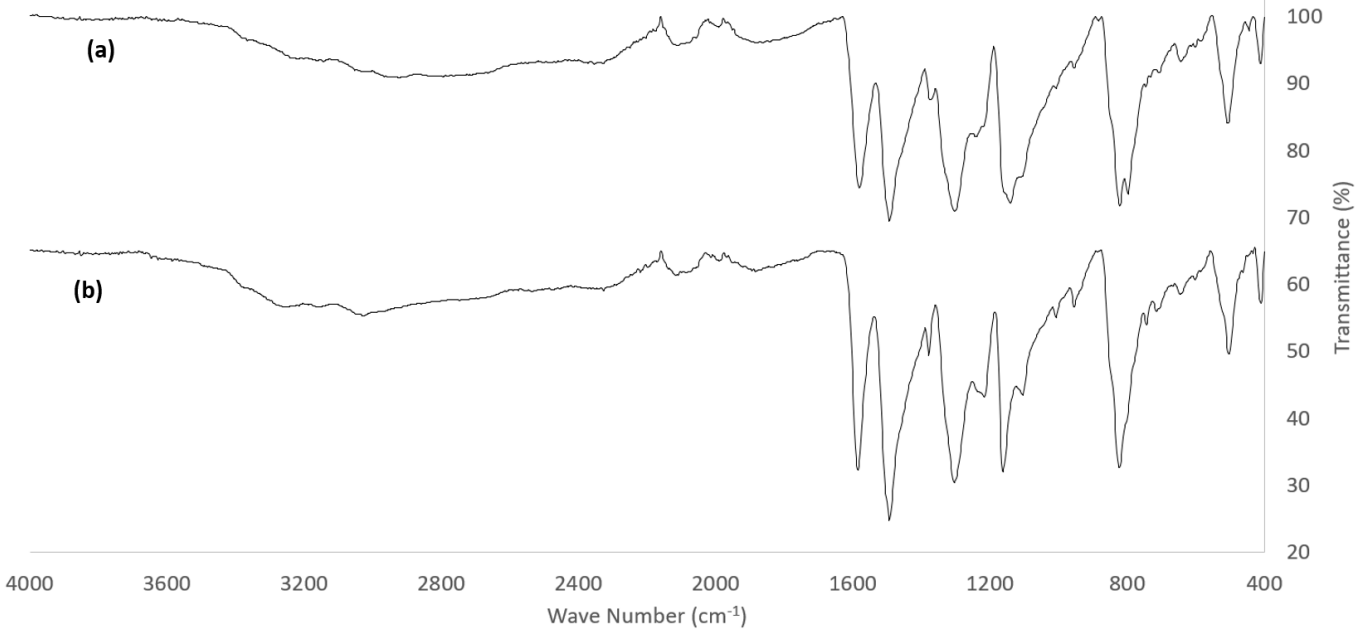

Figure 26. A comparison of the IR spectra of two samples synthesized at -10°C (a) being analyzed after dedoping and (b) having undergone soxhlet extraction.

Table 5

Characteristic PANI Peaks	
1585 cm^{-1}	Quinoid Breathing
1500 cm^{-1}	Benzoid Breathing
1300 cm^{-1}	C-N Stretch of Aromatics
1160 cm^{-1}	Mode of N=Q=N
1140 cm^{-1}	Mode of $Q=\overset{+\bullet}{N}H\text{-}B$ or $B\text{-}\overset{+}{N}H\text{-}B$
820 cm^{-1}	C-H out of plane bend

Table 5. A list of the characteristic peaks of PANI.

CHAPTER 6

CONCLUSION

Properties of PANI films can be altered by variations in the polymers synthesis and preparation and therefore so can PANI's bulk properties. A few examples of possible variations are soxhlet extraction and synthesis temperature which have been shown to affect the molecular weight of the PANI chains.

Soxhlet extraction is frequently employed as a means of washing a polymer sample for long periods of time in the hopes of extracting short chain oligomers from the sample. One effect of this which has been shown in this study is that the process extracts more than the oligomers, also removing residual solvent and dopant left from the synthesis. PANI films which have undergone soxhlet extraction are more conductive when cast into films and doped.

The molecular weight of the synthesized PANI can also be affected by the temperature at which the synthesis was performed. Cooler temperatures slow the aniline initiation process which results in longer polymeric chains. These longer chains make mechanically superior films which are also more electrically conductive.

One final observation from this study is the correlation between crosslinking and chain length. This study shows thermal evidence that longer PANI chains require more energy to crossling in the solid state. This observation is further supported by the fact that this trend has been observed in past, though the observations was not attributed to crosslinking [97].

CHAPTER 7

RECOMMENDATIONS FOR FUTURE WORK

The following are recommended for further research in this area:

1. Further study of the effect of soxhlet extraction with analysis via TGA with evolved gas analysis. In numerous pieces of literature on the subject of heating PANI, it is assumed that weight loss below 100°C is due to loss of solvent. While the loss of solvent may be involved, the fact that conductivity is reversibly lost when HCl doped ES is heated to 100°C indicates that loss of dopant occurs as well. This analysis technique would also reveal whether methanol replaces the water as the trapped solvent or extracts a portion of the water without becoming trapped itself. In case of the former, a new solvent could be used with even less affinity than methanol resulting in a sample with less interstitial solvent and higher crystallinity.
2. Further studies should be done on the crosslinking of PANI.
    a. Studies centered around the analysis of crosslinked PANI in order to determine a definite structure of the crosslinked polymer and, ideally, the mechanism behind the process.
    b. Studies on the rate of crosslinking at varying temperatures. If crosslinking occurs at fairly low temperatures such as those attained in the environment, it would severely limit the potential applications of the polymer to those in climate-controlled, indoor areas.
    c. If crosslnking does prove problematic at atmospheric temperatures, methods of avoiding crosslinking should be developed. It has been shown in this study that

longer, more crystalline PANI chains require more energy to crosslink. This may be a starting point to develop PANI which is more resistant to crosslinking.

REFERENCES

(1) Scherr, E. M.; MacDiarmid, A. G.; Manohar, S. K.; Masters, J. G.; Sun, Y.; Tang, X.; Druy, M. A.; Glatkowski, P. J.; Cajipe, V. B.; Fischer, J. E.; Cromack, K. R.; Jozefowicz, M. E.; Ginder, J. M.; McCall, R. P.; Epstein, A. J., Polyaniline: Oriented films and fibers. *Synthetic Metals* **1991,** *41* (1), 735-738.

(2) Shirakawa, H., The Discovery of Polyacetylene Film: The Dawning of an Era of Conducting Polymers (Nobel Lecture). *Angewandte Chemie International Edition* **2001,** *40* (14), 2574-2580.

(3) Fox Richard, T.; Wani, V.; Howard Kevin, E.; Bogle, A.; Kempel, L., Conductive polymer composite materials and their utility in electromagnetic shielding applications. *Journal of Applied Polymer Science* **2007,** *107* (4), 2558-2566.

(4) Falcon 9Capabilities and Services. SpaceX, Ed. SpaceX: Hawthorne, California, 2018.

(5) Epstein, A. J., Insulator-Metal Transitions and Metalic State in Conducting Polymers. In *Handbook of Conducting Polymers*, 3 ed.; CRC Press: 6000 Broken Sound Parkway NW, Suite 300, 2007; pp 15-7.

(6) Machui, F.; Langner, S.; Zhu, X.; Abbott, S.; Brabec, C. J., Determination of the P3HT:PCBM solubility parameters via a binary solvent gradient method: Impact of solubility on the photovoltaic performance. *Solar Energy Materials and Solar Cells* **2012,** *100*, 138-146.

(7) Xiao, B.; Tang, A.; Yang, J.; Wei, Z.; Zhou, E., P3HT-Based Photovoltaic Cells with a High Voc of 1.22 V by Using a Benzotriazole-Containing Nonfullerene Acceptor End-Capped with Thiazolidine-2,4-dione. *ACS Macro Letters* **2017,** *6* (4), 410-414.

(8) Marsusi, F.; Fedorov, I.; Gerivani, S., *Improving the Performance of Polythiophene-based Electronic devices by Controlling the Band Gap in the Presence of Graphene*. 2017.

(9) Sirringhaus, H.; Tessler, N.; Friend, R. H., Integrated optoelectronic devices based on conjugated polymers. *Science* **1998,** *280* (5370), 1741-4.

(10) Bao, Z.; Dodabalapur, A.; Lovinger, A. J., Soluble and processable regioregular poly(3-hexylthiophene) for thin film field-effect transistor applications with high mobility. *Applied Physics Letters* **1996,** *69* (26), 4108-4110.

(11) Brixi, S.; Melville, O. A.; Boileau, N. T.; Lessard, B. H., The Influence of Air and Temperature on the Performance of PBDB-T and P3HT in Organic Thin Film Transistors. *Journal of Materials Chemistry C* **2018**.

(12) Murphy, A. R.; Liu, J.; Luscombe, C.; Kavulak, D.; Fréchet, J. M. J.; Kline, R. J.; McGehee, M. D., Synthesis, Characterization, and Field-Effect Transistor Performance of Carboxylate-Functionalized Polythiophenes with Increased Air Stability. *Chemistry of Materials* **2005,** *17* (20), 4892-4899.

(13) Lee, S.; Borrelli, D. C.; Gleason, K. K., Air-stable polythiophene-based thin film transistors processed using oxidative chemical vapor deposition: Carrier transport and channel/metallization contact interface. *Organic Electronics* **2016,** *33*, 253-262.

(14) Kazarinoff, P. D.; Shamburger, P. J.; Ohuchi, F. S.; Luscombe, C. K., OTFT performance of air-stable ester-functionalized polythiophenes. *Journal of Materials Chemistry* **2010,** *20* (15), 3040-3045.

(15) Letheby, H., XXIX.-On the production of a blue substance by the electrolysis of sulphate of aniline. *Journal of the Chemical Society* **1862,** *15* (0), 161-163.

(16) Norden, B. *The Nobel Proze in Chemistry, 2000: Conducting Polymers*; The Royal Swedish Academy of Sciences: Stockholm, Sweden 2000.

(17) Wang, Y.; Wang, W.; Ma, Z., Core-shell structural S@polyaniline/SiO2 composite cathodes for lithium-sulfur batteries. *Mater. Focus* **2017,** *6* (6), 678-684.
(18) Tabrizi, A. G.; Arsalani, N.; Naghshbandi, Z.; Ghadimi, L. S.; Mohammadi, A., Growth of polyaniline on rGO-Co3S4 nanocomposite for high-performance supercapacitor energy storage. *Int. J. Hydrogen Energy* **2018**, Ahead of Print.
(19) Mello, H. J. N. P. D.; Mulato, M., PANI/PPY blend thin films electrodeposited for use in EGFET sensors. *J. Appl. Polym. Sci.* **2018**, Ahead of Print.
(20) Kolla, H. S.; Surwade, S. P.; Zhang, X.; MacDiarmid, A. G.; Manohar, S. K., Absolute Molecular Weight of Polyaniline. *Journal of the American Chemical Society* **2005,** *127* (48), 16770-16771.
(21) Ramamurthy, P. C.; Malshe, A. M.; Harrell, W. R.; Gregory, R. V.; McGuire, K.; Rao, A. M., Polyaniline/single-walled carbon nanotube composite electronic devices. *Solid-State Electronics* **2004,** *48* (10), 2019-2024.
(22) Tzou, K.; Gregory, R. V., Kinetic study of the chemical polymerization of aniline in aqueous solutions. *Synthetic Metals* **1992,** *47* (3), 267-277.
(23) Genies, E. M.; Tsintavis, C., Redox mechanism and electrochemical behaviour or polyaniline deposits. *Journal of Electroanalytical Chemistry and Interfacial Electrochemistry* **1985,** *195* (1), 109-128.
(24) Arnautov, S. A.; Zaitsev-Zotov, S. V.; Kobryanskii, V. M., New dopant-solvent system for conductive PAN films production. *Synth. Met.* **1997,** *84* (1-3), 133-134.
(25) Ullah, R.; Ullah, H.; Shah, A.-u.-H. A.; Bilal, S.; Ali, K., Oligomeric synthesis and density functional theory of leucoemeraldine base form of polyaniline. *J. Mol. Struct.* **2017,** *1127*, 734-741.
(26) Jain, R.; Gregory, R. V., Solubility and rheological characterization of polyaniline base in N-methyl-2-pyrrolidinone and N,N′-dimethylpropylene urea. *Synthetic Metals* **1995,** *74* (3), 263-266.
(27) Chacko, A. P.; Hardaker, S. S.; Gregory, R. V.; Hanks, T. W., Melting transition in the leucoemeraldine form of polyaniline. *Polymer* **1998,** *39* (14), 3289-3293.
(28) Leng, J. M.; Ginder, J. M.; McCall, R. P.; Ye, H. J.; Epstein, A. J.; Sun, Y.; Manohar, S. K.; Macdiarmid, A. G., Photoexcitation spectroscopy of pernigraniline. *Synthetic Metals* **1991,** *41* (3), 1311-1314.
(29) Alemán, C.; Ferreira, C. A.; Torras, J.; Meneguzzi, A.; Canales, M.; Rodrigues, M. A. S.; Casanovas, J., On the molecular properties of polyaniline: A comprehensive theoretical study. *Polymer* **2008,** *49* (23), 5169-5176.
(30) Lin, Y.; Mo, D.; Gong, K.; Zhang, G., Ellipsometric spectra of conducting polyaniline. *Acta Phys. Sin. (Overseas Ed.)* **1993,** *2* (11), 816-24.
(31) Cao, Y.; Smith, P.; Heeger, A. J., Counter-ion induced processibility of conducting polyaniline and of conducting polyblends of polyaniline in bulk polymers. *Synthetic Metals* **1992,** *48* (1), 91-97.
(32) Travain, S. A.; Bianchi, R. F.; Colella, E. M. L.; de Andrade, A. M.; Giacometti, J. A., Flexible polyaniline devices for strain gauge and pH monitoring applications. *Polim.: Cienc. Tecnol.* **2007,** *17* (4), 334-338.
(33) Wang, C. In *Nanodevices based on electrospun nanofibers*, American Chemical Society: 2014; pp PMSE-137.
(34) Zhou, X. Transparent conductive film material for circuit board and its manufacture method. CN106531291A, 2017.

(35) Kwon, O.; McKee, M. L., Calculations of Band Gaps in Polyaniline from Theoretical Studies of Oligomers. *The Journal of Physical Chemistry B* **2000,** *104* (8), 1686-1694.
(36) Adams, P. N.; Laughlin, P. J.; Monkman, A. P.; Bernhoeft, N., A further step towards stable organic metals. Oriented films of polyaniline with high electrical conductivity and anisotropy. *Solid State Communications* **1994,** *91* (11), 875-878.
(37) Soos, Z.; Mukhopadhyay, D.; Painelli, A.; Girlando, A., *Handbook of Conducting Polymers, Second Edition, Revised and Expanded*. 1998; p 165-208.
(38) Li, S.; Cao, Y.; Xue, Z., Soluble polyaniline. *Synthetic Metals* **1987,** *20* (2), 141-149.
(39) Eaiprasertsak, K. Temperature Dependence of Electrical Conductivity and Thermoelectric Power in Polyaniline Fibers and Films. Clemson University, Clemson, SC, 1998.
(40) Tsymbal, E. Y., Electronic Trnsport. Lincoln Nebraska, 2008; p 12.
(41) Le, T.-H.; Kim, Y.; Yoon, H., Electrical and Electrochemical Properties of Conducting Polymers. *Polymers* **2017,** *9* (4).
(42) Ohsawa, T.; Kimura, O.; Onoda, M.; Yoshino, K., An ESR study on polyaniline in nonaqueous electrolyte. *Synthetic Metals* **1992,** *47* (2), 151-156.
(43) Horowitz, G.; Yassar, A.; von Bardeleben, H. J., ESR and optical spectroscopy evidence for a chain-length dependence of the charged states of thiophene oligomers. Extrapolation to polythiophene. *Synthetic Metals* **1994,** *62* (3), 245-252.
(44) Brédas, J. L.; Wudl, F.; Heeger, A. J., Polarons and bipolarons in doped polythiophene: A theoretical investigation. *Solid State Communications* **1987,** *63* (7), 577-580.
(45) Mahani, M. R.; Mirsakiyeva, A.; Delin, A., Breakdown of Polarons in Conducting Polymers at Device Field Strengths. *The Journal of Physical Chemistry C* **2017,** *121* (19), 10317-10324.
(46) Liang, X.; Govindaraju, S.; Yun, K., Dual Applicability of Polyaniline Coated Gold Nanorods: A Study of Antibacterial and Redox Activity. *BioChip Journal* **2018**.
(47) Prasankumar, T.; Wiston, B. R.; Gautam, C. R.; Ilangovan, R.; Jose, S. P., Synthesis and enhanced electrochemical performance of PANI/Fe3O4 nanocomposite as supercapacitor electrode. *Journal of Alloys and Compounds* **2018,** *757*, 466-475.
(48) Jafarian, M.; Afghahi, S. S. S.; Atassi, Y.; Salehi, M., Enhanced microwave absorption characteristics of nanocomposite based on hollow carbonyl iron microspheres and polyaniline decorated with MWCNTs. *Journal of Magnetism and Magnetic Materials* **2018,** *462*, 153-159.
(49) Karim, M. R.; Yeum, J. H.; Lee, M. S.; Lim, K. T., Preparation of conducting polyaniline/TiO2 composite submicron-rods by the γ-radiolysis oxidative polymerization method. *React. Funct. Polym.* **2008,** *68* (9), 1371-1376.
(50) Mezhuev, Y. O.; Solov'eva, I. V., Size distribution of polyaniline particles in the process of oxidative polymerization of aniline. *Plast. Massy* **2014,** (11-12), 25-26.
(51) Zhang, J.; Zou, F.; Yu, X.; Huang, X.; Qu, Y., Ionic liquid improves the laccase-catalyzed synthesis of water-soluble conducting polyaniline. *Colloid Polym. Sci.* **2014,** *292* (10), 2549-2554.
(52) Ćirić-Marjanović, G., Recent advances in polyaniline research: Polymerization mechanisms, structural aspects, properties and applications. *Synthetic Metals* **2013,** *177*, 1-47.
(53) Marjanović, B.; Juranić, I.; Ćirić-Marjanović, G., Revised Mechanism of Boyland−Sims Oxidation. *The Journal of Physical Chemistry A* **2011,** *115* (15), 3536-3550.
(54) G. Ciric -Marjanovic, M. T., J. Stejskal, MNDO-PM3 Study of the Early Stages of the Chemical Oxidative Polymerization of Aniline. *Collection of Czech. Chem. Commun.* **2006,** *71* (10), 20.

(55) Behrman, E. J., Studies on the reaction between peroxydisulfate ions and aromatic amines. Boyland-Sims oxidation. *Journal of the American Chemical Society* **1967,** *89* (10), 2424-2428.
(56) Shim, Y. B.; Won, M. S.; Park, S. M., Electrochemistry of Conductive Polymers VIII: In Situ Spectroelectrochemical Studies of Polyaniline Growth Mechanisms. *Journal of The Electrochemical Society* **1990,** *137* (2), 538-544.
(57) Bacon, J.; Adams, R. N., Anodic oxidations of aromatic amines. III. Substituted anilines in aqueous media. *Journal of the American Chemical Society* **1968,** *90* (24), 6596-6599.
(58) Ohsaka, T.; Ohnuki, Y.; Oyama, N.; Katagiri, G.; Kamisako, K., IR absorption spectroscopic identification of electroactive and electroinactive polyaniline films prepared by the electrochemical polymerization of aniline. *Journal of Electroanalytical Chemistry and Interfacial Electrochemistry* **1984,** *161* (2), 399-405.
(59) Gospodinova, N.; Terlemezyan, L., Conducting polymers prepared by oxidative polymerization: polyaniline. *Progress in Polymer Science* **1998,** *23* (8), 1443-1484.
(60) Ding, Y.; Buyle Padias, A.; Hall, H. K., Chemical trapping experiments support a cation-radical mechanism for the oxidative polymerization of aniline. *Journal of Polymer Science Part A: Polymer Chemistry* **2000,** *37* (14), 2569-2579.
(61) Gordana Ćirić-Marjanovića, M. T., Jaroslav Stejskalb,, MNDO-PM3 Study of the Early Stages of the Chemical Oxidative Polymerization of Aniline. *Collect. Czech. Chem. Commun.* **2006,** *71* (10), 20.
(62) Ćirić-Marjanović, G.; Konyushenko, E. N.; Trchová, M.; Stejskal, J., Chemical oxidative polymerization of anilinium sulfate versus aniline: Theory and experiment. *Synthetic Metals* **2008,** *158* (5), 200-211.
(63) Perkin, W. H., LXXIV.-On mauveine and allied colouring matters. *Journal of the Chemical Society, Transactions* **1879,** *35* (0), 717-732.
(64) Travis, A. S., Perkin's Mauve: Ancestor of the Organic Chemical Industry. *Technology and Culture* **1990,** *31* (1), 51-82.
(65) Mezhuev, Y. O.; Korshak, Y. V.; Shtil'man, M. I., A new concept of the kinetics and mechanism of the oxidative polymerization of aromatic amines. *Russian Journal of Physical Chemistry B* **2015,** *9* (2), 306-315.
(66) Wei, Y.; Sun, Y.; Tang, X., Autoacceleration and kinetics of electrochemical polymerization of aniline. *The Journal of Physical Chemistry* **1989,** *93* (12), 4878-4881.
(67) I. Yu. Sapurinaa, J. S., The effect of pH on the oxidative polymerization of aniline and the morphology and properties of products *Russ. Chem. Rev.* **2010,** *79* (12), 22.
(68) Cavallo Pablo, C.; Muñoz Diego, J.; Miras Maria, C.; Barbero, C.; Acevedo Diego, F., Extracting kinetic parameters of aniline polymerization from thermal data of a batch reactor. simulation of the thermal behavior of a reactor. *Journal of Applied Polymer Science* **2013,** *131* (4).
(69) Al-Nasassrah, M. A.; Podczeck, F.; Newton, J. M., The effect of an increase in chain length on the mechanical properties of polyethylene glycols. *European Journal of Pharmaceutics and Biopharmaceutics* **1998,** *46* (1), 31-38.
(70) Effect of Molecular Weight on Polymeric Properties. In *Polymer Properties Database*, Polymer Properties Database: 2015.
(71) Chinn, D.; Janata, J., Spin-cast thin films of polyaniline. *Thin Solid Films* **1994,** *252* (2), 145-151.

(72) Tian, W. Effects of Draw Ratio and Dopant on Electrically Conductive Polyaniline. Clemson, Clemson, 1999.
(73) Begum, A. N.; Dhachanamoorthi, N.; saravanan, M. E. R.; Jayamurugan, P.; Manoharan, D.; Ponnuswamy, V., Influence of annealing effects on polyaniline for good microstructural modification. *Optik - International Journal for Light and Electron Optics* **2013,** *124* (3), 238-242.
(74) Ramamurthy, P. C.; Harrell, W. R.; Gregory, R. V.; Sadanadan, B.; Rao, A. M., Mechanical and Electrical Properties of Solution-Processed Polyaniline/Multiwalled Carbon Nanotube Composite Films. *Journal of The Electrochemical Society* **2004,** *151* (8), G502-G506.
(75) Yang, Y.; Chen, S.; Xu, L., Enhanced Conductivity of Polyaniline by Conjugated Crosslinking. *Macromolecular Rapid Communications* **2011,** *32* (7), 593-597.
(76) MacDiarmid, A. G.; Min, Y.; Wiesinger, J. M.; Oh, E. J.; Scherr, E. M.; Epstein, A. J., Towards optimization of electrical and mechanical properties of polyaniline: Is crosslinking between chains the key? *Synthetic Metals* **1993,** *55* (2), 753-760.
(77) Chen, S. A.; Lee, H. T., Polyaniline plasticized with 1-methyl-2-pyrrolidone: structure and doping behavior. *Macromolecules* **1993,** *26* (13), 3254-3261.
(78) Mathew, R.; Mattes, B. R.; Espe, M. P., A solid state NMR characterization of cross-linked polyaniline powder. *Synthetic Metals* **2002,** *131* (1), 141-147.
(79) Luo, K.; Shi, N.; Sun, C., Thermal transition of electrochemically synthesized polyaniline. *Polymer Degradation and Stability* **2006,** *91* (11), 2660-2664.
(80) Ozawa, T., A new method of analysing thermogravimetric data. *Bulletin of the Chemical Society of Japan* **1965,** *38* (11), 1881-1886.
(81) Kissinger, H. E., Reaction Kinetics in Differential Thermal Analysis. *Analytical Chemistry* **1957,** *29* (11), 1702-1706.
(82) Tan, H. H.; Neoh, K. G.; Liu, F. T.; Kocherginsky, N.; Kang, E. T., Crosslinking and its effects on polyaniline films. *Journal of Applied Polymer Science* **2001,** *80* (1), 1-9.
(83) Ansari, R.; Price, W. E.; Wallace, G. G., Effect of thermal treatment on the electroactivity of polyaniline. *Polymer* **1996,** *37* (6), 917-923.
(84) Lee, J.-S.; Mohammad, C.; Koh, H.-D.; Shashadhar, S.; Kang, N.-G.; Shin, W.-J.; Kim, Y.-J. Supramolecular polymeric structure of having sub-nano scale ordering. WO2009139513A1, 2009.
(85) Shi, M.; Zhang, Y.; Bai, M.; Li, B., Facile fabrication of polyaniline with coral-like nanostructure as electrode material for supercapacitors. *Synthetic Metals* **2017,** *233*, 74-78.
(86) Sapurina, I.; Shishov, M. A., *Oxidative Polymerization of Aniline: Molecular Synthesis of Polyaniline and the Formation of Supramolecular Structures*. 2012; p 251-312.
(87) Liu, J. Core-shell structure of nickel oxide/poly aniline supercapacitor electrode material and preparation method thereof [Machine Translation]. CN108010727A, 2018.
(88) Lin, Q.; Zhang, X. Preparation method of ultra-thin wall multistage and porous carbons/polyaniline supercapacitor electrode materials [Machine Translation]. CN108010750A, 2018.
(89) Wang, H. Preparation method of Co3O4-Si-C-polyaniline anode material for lithium ion air battery. CN107134580A, 2017.
(90) Lodha, A.; Kilbey, S. M.; Ramamurthy Praveen, C.; Gregory Richard, V., Effect of annealing on electrical conductivity and morphology of polyaniline films. *Journal of Applied Polymer Science* **2001,** *82* (14), 3602-3610.

(91) Allin, S. B., Polymer Science and Technology, 2nd Edition (Joel R. Fried). *Journal of Chemical Education* **2004,** *81* (6), 809.
(92) Li, J.; Tang, X.; Li, H.; Yan, Y.; Zhang, Q., Synthesis and thermoelectric properties of hydrochloric acid-doped polyaniline. *Synthetic Metals* **2010,** *160* (11), 1153-1158.
(93) MacDiarmid, A. G.; Epstein, A. J., The concept of secondary doping as applied to polyaniline. *Synthetic Metals* **1994,** *65* (2), 103-116.
(94) Sanches, E. A.; Soares, J. C.; Mafud, A. C.; Fernandes, E. G. R.; Leite, F. L.; Mascarenhas, Y. P., Structural characterization of Chloride Salt of conducting polyaniline obtained by XRD, SAXD, SAXS and SEM. *Journal of Molecular Structure* **2013,** *1036*, 121-126.
(95) Berner, D.; Davenas, J.; Djurado, D.; Nechtschein, M.; Rannou, P.; Travers, J. P., Annealing effect in polyaniline-CSA upon moderate heating. *Synthetic Metals* **1999,** *101* (1), 727-728.
(96) Sinha, S.; Bhadra, S.; Khastgir, D., Effect of dopant type on the properties of polyaniline. *Journal of Applied Polymer Science* **2009,** *112* (5), 3135-3140.
(97) Beadle, P. M.; Nicolau, Y. F.; Banka, E.; Rannou, P.; Djurado, D., Controlled polymerization of aniline at sub-zero temperatures. *Synthetic Metals* **1998,** *95* (1), 29-45.
(98) Oh, E. J.; Min, Y.; Wiesinger, J. M.; Manohar, S. K.; Scherr, E. M.; Prest, P. J.; MacDiarmid, A. G.; Epstein, A. J., Polyaniline: Dependency of selected properties on molecular weight. *Synthetic Metals* **1993,** *55* (2), 977-982.
(99) Tang, J.; Jing, X.; Wang, B.; Wang, F., Infrared spectra of soluble polyaniline. *Synthetic Metals* **1988,** *24* (3), 231-238.
(100) Salaneck, W. R.; Liedberg, B.; Inganäs, O.; Erlandsson, R.; Lundström, I.; Macdiarmid, A. G.; Halpern, M.; Somasiri, N. L. D., Physical Characterization of Some Polyaniline, (øN)x. *Molecular Crystals and Liquid Crystals* **1985,** *121* (1-4), 191-194.
(101) Gruger, A.; Novak, A.; Régis, A.; Colomban, P., Infrared and Raman study of polyaniline Part II: Influence of ortho substituents on hydrogen bonding and UV/Vis—near-IR electron charge transfer. *Journal of Molecular Structure* **1994,** *328*, 153-167.
(102) McCall, R. P.; Roe, M. G.; Ginder, J. M.; Kusumoto, T.; Epstein, A. J.; Asturias, G. E.; Scherr, E. M.; MacDiarmid, A. G., IR absorption, photoinduced IR absorption, and photoconductivity of polyaniline. *Synthetic Metals* **1989,** *29* (1), 433-438.
(103) Li, G.; Zhang, Z., Synthesis of Dendritic Polyaniline Nanofibers in a Surfactant Gel. *Macromolecules* **2004,** *37* (8), 2683-2685.

VITA

Samuel Watson Stahl
4541 Hampton Boulevard
Norfolk, VA 23529-0126
swatsonstahl@gmail.com
(757) 683-4078

EDUCATION

M.S. in Chemistry

Old Dominion University
Department of Chemistry and Biochemistry
4541 Hampton Boulevard
Norfolk, VA 23529-0126
Graduation: August 2018

Research: Determines the effect of soxhlet extraction and synthesis temperature on the electrical conductivity of polyaniline.

Coursework

Advanced Inorganic Chemistry
Advanced Analytical Chemistry
Atmospheric Chemistry
Organic Spectroscopy
Advanced Mass Spectroscopy
Kinetics and Thermodynamics
Mechanical Sensing and Signal Transduction
Environmental Chemistry

B.S. in Chemistry (ACS Certified)
Mathematics Minor
James Madison University
Department of Chemistry and Biochemistry
800 South Main Street
Harrisonburg, VA 22807
Graduation: May 2016

Research: Designed and produced microfluidic devices to be used in public school to promote scientific concepts. Developed methods to promote adhesion of gold to polymer substrates.

Coursework (In addition to courses required for ACS Certification)

Science of the Small (Nanotechnology Topics Course)
Polymer Chemistry
Selection and Use of Engineering Materials
Intro to Materials Science
Intermediate Organic Chemistry

EXPERIENCE

Graduate Teaching Assistant
Aug. 2016 – May 2018
Old Dominion University
Norfolk, VA 23529-0126

Undergraduate Researcher
Jan. 2014 – July 2016
James Madison University
Harrisonburg, VA 22807

The word processor for this thesis was Microsoft Word 2016. All graphs were made using Microsoft Excel 2016 unless otherwise specified. Molecular structures were drawn using ChemDraw Professional 16.0.